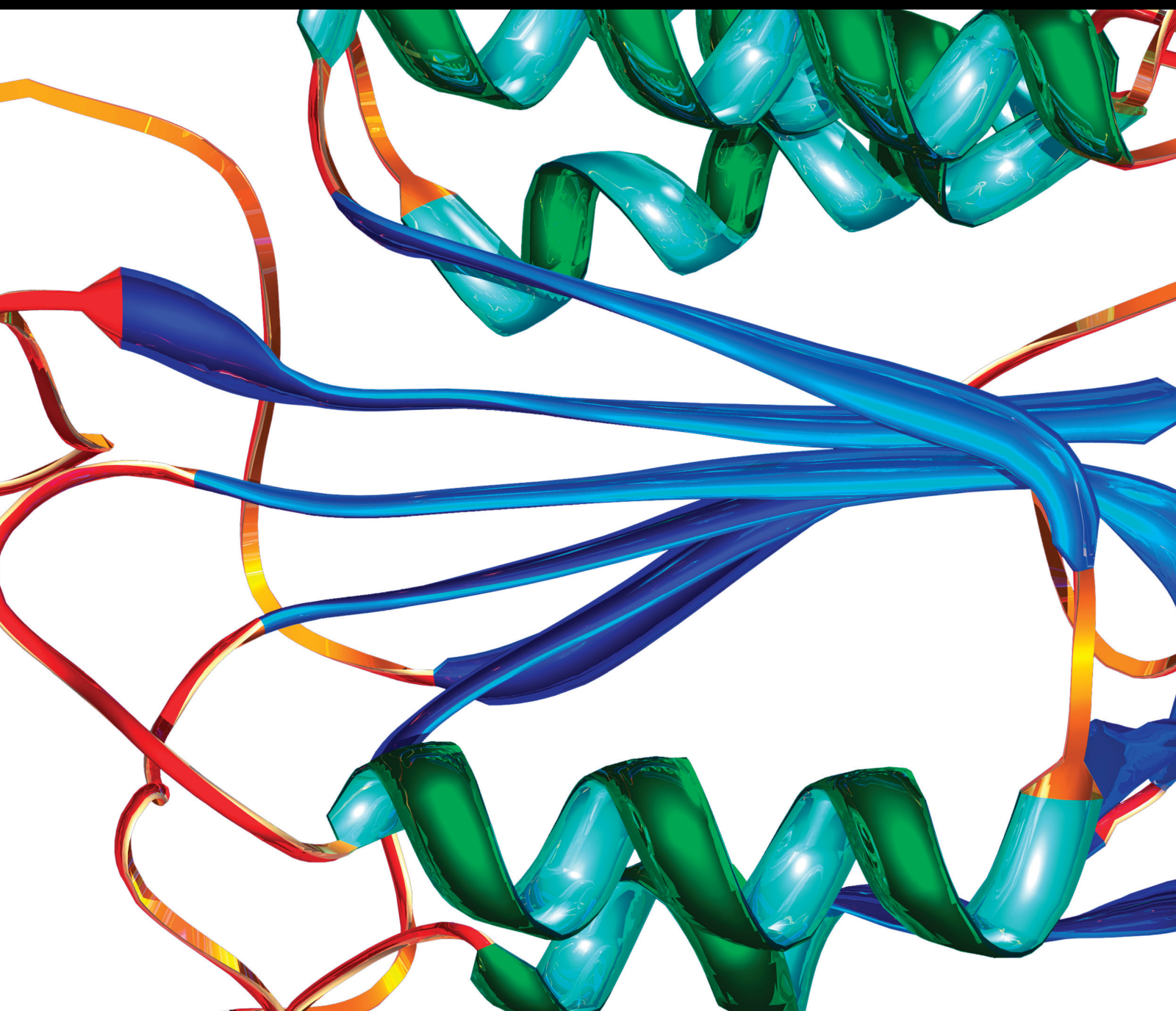


# Emerging Biomarkers in Genitourinary Cancer

Lead Guest Editor: Giovanni Cochetti

Guest Editors: Oommen P. Oommen and Matteo Giulietti





---

# **Emerging Biomarkers in Genitourinary Cancer**



Disease Markers

---

## **Emerging Biomarkers in Genitourinary Cancer**

Lead Guest Editor: Giovanni Cochetti

Guest Editors: Oommen P. Oommen and Matteo  
Giulietti



---


Copyright © 2019 Hindawi Limited. All rights reserved.

This is a special issue published in "Disease Markers." All articles are open access articles distributed under the Creative Commons Attribution License, which permits unrestricted use, distribution, and reproduction in any medium, provided the original work is properly cited.



# Chief Editor

Paola Gazzaniga, Italy




## Associate Editors

Donald H. Chace , USA  
Mariann Harangi, Hungary  
Hubertus Himmerich , United Kingdom  
Yi-Chia Huang , Taiwan  
Giuseppe Murdaca , Italy  
Irene Rebelo , Portugal

## Academic Editors

Muhammad Abdel Ghafar, Egypt  
George Agrogiannis, Greece  
Mojgan Alaeddini, Iran  
Atif Ali Hashmi , Pakistan  
Cornelia Amalinei , Romania  
Pasquale Ambrosino , Italy  
Paul Ashwood, USA  
Faryal Mehwish Awan , Pakistan  
Atif Baig , Malaysia  
Valeria Barresi , Italy  
Lalit Batra , USA  
Francesca Belardinilli, Italy  
Elisa Belluzzi , Italy  
Laura Bergantini , Italy  
Sourav Bhattacharya, USA  
Anna Birková , Slovakia  
Giulia Bivona , Italy  
Luisella Bocchio-Chiavetto , Italy  
Francesco Paolo Busardó , Italy  
Andrea Cabrera-Pastor , Spain  
Paolo Cameli , Italy  
Chiara Caselli , Italy  
Jin Chai, China  
Qixing Chen, China  
Shaoqiu Chen, USA  
Xiangmei Chen, China  
Carlo Chiarla , Italy  
Marcello Ciaccio , Italy  
Luciano Colangelo , Italy  
Alexandru Corlateanu, Moldova  
Miriana D'Alessandro , Saint Vincent and the Grenadines  
Waaqo B. Daddacha, USA  
Xi-jian Dai , China  
Maria Dalamaga , Greece

Serena Del Turco , Italy  
Jiang Du, USA  
Xing Du , China  
Benoit Dugue , France  
Paulina Dumnicka , Poland  
Nashwa El-Khazragy , Egypt  
Zhe Fan , China  
Rudy Foddis, Italy  
Serena Fragiotta , Italy  
Helge Frieling , Germany  
Alain J. Gelibter, Italy  
Matteo Giulietti , Italy  
Damjan Glavač , Slovenia  
Alvaro González , Spain  
Rohit Gundamaraju, USA  
Emilia Hadziyannis , Greece  
Michael Hawkes, Canada  
Shih-Ping Hsu , Taiwan  
Menghao Huang , USA  
Shu-Hong Huang , China  
Xuan Huang , China  
Ding-Sheng Jiang , China  
Esteban Jorge Galarza , Mexico  
Mohamed Gomaa Kamel, Japan  
Michalis V. Karamouzis, Greece  
Muhammad Babar Khawar, Pakistan  
Young-Kug Kim , Republic of Korea  
Mallikarjuna Korivi , China  
Arun Kumar , India  
Jinan Li , USA  
Peng-fei Li , China  
Yiping Li , China  
Michael Lichtenauer , Austria  
Daniela Ligi, Italy  
Hui Liu, China  
Jin-Hui Liu, China  
Ying Liu , USA  
Zhengwen Liu , China  
César López-Camarillo, Mexico  
Xin Luo , USA  
Zhiwen Luo, China  
Valentina Magri, Italy  
Michele Malaguarnera , Italy  
Erminia Manfrin , Italy  
Utpender Manne, USA




Alexander G. Mathioudakis, United Kingdom  
Andrea Maugeri , Italy  
Prasenjit Mitra , India  
Ekansh Mittal , USA  
Hiroshi Miyamoto , USA  
Naoshad Muhammad , USA  
Chiara Nicolazzo , Italy  
Xing Niu , China  
Dong Pan , USA  
Dr.Krupakar Parthasarathy, India  
Robert Pichler , Austria  
Dimitri Poddighe , Kazakhstan  
Roberta Rizzo , Italy  
Maddalena Ruggieri, Italy  
Tamal Sadhukhan, USA  
Pier P. Sainaghi , Italy  
Cristian Scheau, Romania  
Jens-Christian Schewe, Germany  
Alexandra Scholze , Denmark  
Shabana , Pakistan  
Anja Hviid Simonsen , Denmark  
Eric A. Singer , USA  
Daniele Sola , Italy  
Timo Sorsa , Finland  
Yaying Sun , China  
Mohammad Tarique , USA  
Jayaraman Tharmalingam, USA  
Sowjanya Thatikonda , USA  
Stamatios E. Theocharis , Greece  
Tilman Todenhöfer , Germany  
Anil Tomar, India  
Alok Tripathi, India  
Drenka Trivanović , Germany  
Natacha Turck , Switzerland  
Azizah Ugusman , Malaysia  
Shailendra K. Verma, USA  
Aristidis S. Veskoukis, Greece  
Arianna Vignini, Italy  
Jincheng Wang, Japan  
Zhongqiu Xie, USA  
Yuzhen Xu, China  
Zhijie Xu , China  
Guan-Jun Yang , China  
Yan Yang , USA

Chengwu Zeng , China  
Jun Zhang Zhang , USA  
Qun Zhang, China  
Changli Zhou , USA  
Heng Zhou , China  
Jian-Guo Zhou, China

## Contents

---

### **Proteomic Comparison of Malignant Human Germ Cell Tumor Cell Lines**

Felix Bremmer , Hanibal Bohnenberger , Stefan Küffer, Thomas Oellerich, Hubert Serve, Henning Urlaub, Arne Strauss, Yasmine Maatoug, Carl Ludwig Behnes, Christoph Oing, Heinz Joachim Radzun, Philipp Ströbel, Stefan Balabanov, and Friedemann Honecker 










Research Article (14 pages), Article ID 8298524, Volume 2019 (2019)

### **De Ritis Ratio (Aspartate Transaminase/Alanine Transaminase) as a Significant Prognostic Factor in Patients Undergoing Radical Cystectomy with Bladder Urothelial Carcinoma: A Propensity Score-Matched Study**

Hyeong Dong Yuk , Chang Wook Jeong, Cheol Kwak, Hyeon Hoe Kim, and Ja Hyeon Ku 



Research Article (8 pages), Article ID 6702964, Volume 2019 (2019)

### **CSF-1 Overexpression Predicts Poor Prognosis in Upper Tract Urothelial Carcinomas**

Wei-Chi Hsu , Yi-Chen Lee , Peir-In Liang, Lin-Li Chang , A-Mei Huang , Hui-Hui Lin , Wen-Jeng Wu , Ching-Chia Li , Wei-Ming Li, Jhen-Hao Jhan , and Hung-Lung Ke 

Research Article (9 pages), Article ID 2724948, Volume 2019 (2019)

### **The Prognostic Significance of Protein Expression of CASZ1 in Clear Cell Renal Cell Carcinoma**

Bohyun Kim , Minsun Jung, and Kyung Chul Moon 

Research Article (6 pages), Article ID 1342161, Volume 2019 (2019)



## Research Article

# Proteomic Comparison of Malignant Human Germ Cell Tumor Cell Lines

**Felix Bremmer**<sup>1</sup>, **Hanibal Bohnenberger**<sup>1</sup>, **Stefan Küffer**<sup>1</sup>, **Thomas Oellerich**<sup>2,3</sup>,  
**Hubert Serve**<sup>2,3</sup>, **Henning Urlaub**<sup>4,5</sup>, **Arne Strauss**<sup>6</sup>, **Yasmine Maatoug**<sup>1</sup>, **Carl Ludwig Behnes**<sup>1</sup>,  
**Christoph Oing**<sup>7</sup>, **Heinz Joachim Radzun**<sup>1</sup>, **Philipp Ströbel**<sup>1</sup>, **Stefan Balabanov**<sup>8</sup>,  
and **Friedemann Honecker**<sup>7,9</sup>

<sup>1</sup>Institute of Pathology, University Medical Center, Robert-Koch-Str. 40, 37075 Göttingen, Germany

<sup>2</sup>Department of Medicine II, Hematology/Oncology, Goethe University, Theodor-Stern-Kai 7, 60590 Frankfurt, Germany

<sup>3</sup>German Cancer Research Center and German Cancer Consortium, 69120 Heidelberg, Germany

<sup>4</sup>Bioanalytical Mass Spectrometry Group, Max Planck Institute for Biophysical Chemistry, Am Fassberg 11, 37077 Göttingen, Germany

<sup>5</sup>Bioanalytics, University Medical Center, Robert-Koch-Str. 40, 37075 Göttingen, Germany

<sup>6</sup>Department of Urology, University Medical Center, Robert-Koch-Str. 40, 37075 Göttingen, Germany

<sup>7</sup>Department of Oncology, Hematology and Bone Marrow Transplantation with Section of Pneumology, University Medical Center Hamburg-Eppendorf, Martinistraße 52, 20246 Hamburg, Germany

<sup>8</sup>Division of Hematology, University Hospital Zurich, Rämistrasse 100, 8091 Zürich, Switzerland

<sup>9</sup>Tumour and Breast Center ZeTuP St. Gallen, Rorschacher Strasse 150, 9006 St. Gallen, Switzerland

Correspondence should be addressed to Felix Bremmer; [felix.bremmer@med.uni-goettingen.de](mailto:felix.bremmer@med.uni-goettingen.de)

Received 25 February 2019; Revised 10 May 2019; Accepted 25 June 2019; Published 3 September 2019

Guest Editor: Oommen P. Oommen

Copyright © 2019 Felix Bremmer et al. This is an open access article distributed under the Creative Commons Attribution License, which permits unrestricted use, distribution, and reproduction in any medium, provided the original work is properly cited. The publication of this article was funded by Max Planck.

Malignant germ cell tumors (GCT) are the most common malignant tumors in young men between 18 and 40 years. The correct identification of histological subtypes, in difficult cases supported by immunohistochemistry, is essential for therapeutic management. Furthermore, biomarkers may help to understand pathophysiological processes in these tumor types. Two GCT cell lines, TCam-2 with seminoma-like characteristics, and NTERA-2, an embryonal carcinoma-like cell line, were compared by a quantitative proteomic approach using high-resolution mass spectrometry (MS) in combination with stable isotope labelling by amino acid in cell culture (SILAC). We were able to identify 4856 proteins and quantify the expression of 3936. 347 were significantly differentially expressed between the two cell lines. For further validation, CD81, CBX-3, PHF6, and ENSA were analyzed by western blot analysis. The results confirmed the MS results. Immunohistochemical analysis on 59 formalin-fixed and paraffin-embedded (FFPE) normal and GCT tissue samples (normal testis, GCNIS, seminomas, and embryonal carcinomas) of these proteins demonstrated the ability to distinguish different GCT subtypes, especially seminomas and embryonal carcinomas. In addition, siRNA-mediated knockdown of these proteins resulted in an antiproliferative effect in TCam-2, NTERA-2, and an additional embryonal carcinoma-like cell line, NCCIT. In summary, this study represents a proteomic resource for the discrimination of malignant germ cell tumor subtypes and the observed antiproliferative effect after knockdown of selected proteins paves the way for the identification of new potential drug targets.

## 1. Introduction

Germ cell tumors (GCT) are the most common malignancies in men between 15 and 40 years of age, and the incidence has constantly increased over the last four decades [1]. Germ cell tumors are histologically and clinically divided into seminomas and nonseminomas. Nonseminomas can be further subdivided into embryonal carcinomas, yolk sac tumors, chorionic carcinomas, and teratomas [2]. Seminomas and nonseminomas have a common precursor called germ cell neoplasia in situ (GCNIS) [3]. The International Germ Cell Cancer Collaborative Group (IGCCCG) developed a prognostic classification system, which divided patients with germ cell tumors into good-, intermediate, and poor-risk groups. It is based besides on several points such as the primary site of the GCT, metastatic sites of involvement, and levels of serum tumor markers in particular upon the histology of the tumors (seminoma versus nonseminoma). Because the treatment of these tumors is different, it is important to differentiate between seminomas and nonseminomas [4]. Patients even with metastasized disease can be cured in about 80% of cases by cisplatin-based chemotherapy [5, 6].

Several cell lines are available as models for the different types of GCT. NTERA-2 and NCCIT display embryonal carcinoma characteristics; meanwhile, TCam-2 is considered a model for seminoma [7, 8]. In this study, we set out to establish new biomarkers for the differentiation of GCT cell lines and formalin-fixed and paraffin-embedded (FFPE) tissue samples and to identify new potential drug targets to improve the therapeutic options especially of patients with embryonal carcinoma.

van der Zwan et al. performed a comprehensive study to identify epigenetic footprints in TCam-2 and NCCIT cell lines. They investigated interactions between gene expression, DNA CpG methylation, and posttranslational histone modifications to elucidate their role in the pathophysiology and etiology of germ cell tumors [9]. However, as the correlation between genetic alterations, RNA expression, and protein expression is highly influenced by transcriptional, translational, and posttranscriptional regulations [10], we aimed for a global, unbiased, and quantitative analysis of the two cell lines TCam-2 and NTERA-2 on the protein level.

With markers such as SALL4, OCT3/4, SOX-2, or SOX-17, numerous good and reliable diagnostic markers are available to differentiate between the different GCT subtypes [2, 11]. Regardless of this, it is of great importance to detect differences in tumor biology in order to gain a better understanding of the pathological processes of germ cell tumors. We reasoned that a proteomic approach, rather than genomic and transcriptomic studies, can identify biological differences and may also provide new potential targets for a molecular targeted therapy. For this purpose, we employed high-resolution mass spectrometric analysis combined with stable isotope labelling with amino acids in cell culture (SILAC) to visualize them in human testis and human germ cell tumor tissue [12]. This strategy can help to minimize variation occurring as a result of sample handling, because the labelling occurs in a very early stage of the experiment [13].

## 2. Material and Methods

**2.1. Culture of TGCT Cell Lines.** In the present study, the human GCT cell lines NTERA-2 (representing an embryonal carcinoma, CRL 1973; from American Type Culture Collection, Manassas, VA, USA), NCCIT (representing an embryonal carcinoma, CRL 2073; from American Type Culture Collection, Manassas, VA, USA), and TCam-2 (representing a seminoma; generously provided by the Department of Developmental Pathology, University of Bonn Medical School, Germany) were cultured in HEPES-buffered RPMI-1640 (Biochrom, Berlin, Germany) supplemented with fetal calf serum (FCS, 10%; CC Pro, Neustadt, Germany), penicillin (100 IU/ml; Sigma-Aldrich, Munich, Germany), streptomycin (100  $\mu$ g/ml; Sigma-Aldrich), and L-glutamine (2 mM; Biochrom, Berlin, Germany). The incubation temperature was 37°C in a humid atmosphere with 5% carbon dioxide in the air.

**2.2. Proteomic Analysis.** Stable isotope labeling with amino acids in cell culture (SILAC) and quantitative mass spectrometry were performed as described before [14–16]. TCam-2 and N-Tera2 cells were cultured in RPMI 1640 medium lacking arginine and lysine (Pierce) supplemented with 10% dialyzed FCS (Invitrogen), 4 mM glutamine, and antibiotics. “Heavy” and “light” media were distinguished by adding 0.115 mM  $^{13}\text{C}_6$   $^{14}\text{N}_4$  L-arginine and 0.275 mM L-lysine-4,4,5,5-D4 (Eurisotop) or equimolar levels of the corresponding nonlabeled (light) amino acids (Merck Millipore), respectively. For cell lysis, 0.5% Nonidet P-40 buffer containing 50 mM Tris/HCl, pH 7.8, 150 mM NaCl, 1 mM  $\text{Na}_3\text{VO}_4$ , 1 mM NaF, 0.2% lauryl maltoside, and protease inhibitors (Complete, Roche) was used. Protein concentration was determined with DC Protein Assay (Bio-Rad) following the manufacturer’s instructions. Equal amounts of protein of light-labeled TCam-2 were mixed with heavy-labeled NTERA-2 and vice versa. Proteins were separated by 1D-PAGE (4 to 12% NuPAGE Bis-Tris Gel, Invitrogen). After Coomassie brilliant blue staining, the gel was divided in 23 slices. Encompassing proteins were reduced with 10 mM DTT for 55 min at 56°C, alkylated with 55 mM IAA for 20 min at 26°C, and gel-digested with modified trypsin (Promega) overnight at 37°C.

Resulting peptides were separated by a C18 precolumn (2.5 cm, 360  $\mu$ m o.d., 100  $\mu$ m i.d., Reprosil-Pur 120 Å, 5  $\mu$ m, C18-AQ, Dr. Maisch GmbH) at a flow rate of 10  $\mu$ l/min and a C18 capillary column (20 cm, 360  $\mu$ m o.d., 75  $\mu$ m i.d., Reprosil-Pur 120 Å, 3  $\mu$ m, C18-AQ, Dr. Maisch GmbH) at a flow rate of 300 nl/min, with a gradient of acetonitrile ranging from 5 to 35% in 0.1% formic acid for 90 min using an Proxeon nano LC coupled to an Q Exactive mass spectrometer (Thermo Electron). MS conditions were as follows: spray voltage, 1.8 kV; heated capillary temperature, 270°C; and normalized collision-energy (NCE), 28. An underfill ratio of 1.2% and intensity threshold of 4.0 e4 were used. The mass spectrometer automatically switched between MS and MS/MS acquisitions (data-dependent mode). Survey MS spectra were acquired in the Orbitrap ( $m/z$  350–1600) with the resolution set to 70 000 at  $m/z$  200 and automatic gain

control target at  $2 \times e^5$ . The 15 most intense ions were sequentially isolated for HCD MS/MS fragmentation and detection. Raw data were analyzed with MaxQuant (version 1.3.0.5) using Uniprot human (version 27.08.2012 with 86725 entries) as a sequence database. Up to two missed cleavages of trypsin were allowed. Oxidized methionine was searched as variable modification and cysteine carbamidomethylation as fixed modification. The modifications corresponding to arginine and lysine labeled with heavy stable isotopes were handled as fixed modifications. The false positive rate was set to 1% at the peptide level, the false discovery rate was set to 1% at the protein level, and the minimum required peptide length was set to six amino acids.

**2.3. Selection of Proteins for Further Investigations.** To see if the proteins detected in the SILAC assays are also expressed in human testis tumor tissue, we compared the significantly expressed proteins of our results with the data in the online database *The Human Protein Atlas* (<https://www.proteinatlas.org/>) [17]. In the selection, we exemplarily opted for proteins that were expressed in tumor-free testicular tissue, with the consideration that these proteins could possibly be of particular importance in testicular tumors.

**2.4. Western Blot Analysis.** Total protein lysates were prepared using RIPA buffer with protease inhibitors (Roche, Germany) and were quantified by the Bio-Rad DC Protein Assay (Bio-Rad, USA). For western blotting, the following primary antibody dilutions were used: monoclonal mouse anti-CD81 (Tetraspanin-28) (Santa Cruz, sc-166029; 1:250), monoclonal mouse anti-PHF6 (PHD finger protein 6) (Santa-Cruz, sc-365237; 1:500), polyclonal rabbit anti-CBX-3 (chromobox protein homolog 3) (HPA 004902, Sigma-Aldrich; 1/250), and polyclonal rabbit anti-ENSA (alpha-endosulfine) (HPA 051292, Sigma-Aldrich: 1/500). Primary antibodies were detected by polyclonal immunoglobulins/HRP secondary antibodies (1:1000, Dako, DK). Membranes were developed using the ECL system (Amersham Bioscience, Germany).

**2.5. Gene Ontology and Network Analysis.** Gene ontology classification has been performed using either the Metacore software (<https://portal.genego.com/>) or the R package clusterProfiler. Differentially expressed proteins were loaded into Metacore software, and significantly enriched biological processes, molecular functions, and pathway networks were extracted.

Network analyses were performed using the Metacore (<https://portal.genego.com/>) software for the enrichment of the shortest pathways inside the group of differentially regulated proteins. The shortest path algorithm connects the differentially expressed proteins identified in the proteomic approach with additional information from the Metacore database along a directed path and potentially involved pathways. Next, most significant networks were loaded into Cytoscape software (<http://www.cytoscape.org/>) for further visualization. Networks were visualized using hierarchical layout in Cytoscape.

**2.6. Tissue Samples of Primary TGCT.** Formalin-fixed and paraffin-embedded tumor tissues of orchiectomy specimens were collected from 59 male patients from the University Medical Centre Göttingen, Germany. Tumors were classified and staged on the basis of the WHO classification [18]. In the present study, a number of 75 blocks have been included. Investigated cases included normal testis adjacent to tumor ( $n = 16$ ), GCNIS ( $n = 18$ ), seminomas ( $n = 21$ ), and embryonal carcinomas ( $n = 20$ ). Ethical approval for using the human material in the present study was obtained from the Ethics Committee of the University Medical Centre Göttingen.

**2.7. Immunohistochemistry.** Immunohistochemical reactions were performed on  $4 \mu\text{m}$  formalin-fixed and paraffin-embedded testis tissue sections. In heat-induced epitope retrieval, the antigen retrieval was carried out at  $98^\circ\text{C}$  in citrate buffer (low pH 6; 40 minutes) or EDTA buffer (high pH 9; 20 minutes). The primary antibodies were incubated for 30 minutes at room temperature. The following antibodies and dilutions were applied: anti-CD81 (mouse, high buffer, 1:200, Santa Cruz, sc-166029), anti-PHF6 (mouse, high buffer, 1:200, Santa-Cruz, sc-365237), anti-CBX-3 (rabbit, diluted 1/200, high buffer, HPA 004902, Sigma-Aldrich), and anti-ENSA (rabbit, diluted 1/50, low buffer, HPA 051292, Sigma-Aldrich). Afterwards, the sections were incubated with a ready-to-use HRP-labeled secondary antibody at room temperature for 25 minutes (anti-rabbit/mouse, produced in goat; Dako REAL EnVision Detection System, DAKO). The substrate DAB+ Chromogen system produces a brown end product and is applied to visualize the site of the target antigen (Dako REAL DAB+ Chromogen, DAKO). Tissue samples were counterstained with Meyer's hematoxylin (Dako) for 8 minutes and were analyzed by light microscopy.

Two independent investigators evaluated all tissue sections stained for CD81, CBX-3, PHF-6, and ENSA using an immunoreactivity staining score (IRS) as described previously [18, 19]. The percentage of positively stained cells was first classified using a 0–4 scoring system: score 0 = 0% positive cells, score 1 = less than 10% positive cells, score 2 = 10–50% positive cells, score 3 = 51–80% positive cells, and score 4 = >80% positive cells. The intensity of staining was evaluated on a four-tiered scale (0 = negative, 1 = weak, 2 = intermediate, and 3 = strong). Afterwards, the scores of intensity and staining were multiplied, and the mean value per patient was calculated, as described previously [18]. Differences of IRS between the different subtypes of GCT were statistically evaluated using Student's *t*-test (GraphPad Software, San Diego, CA, USA). A *p* value of  $<0.05$  was considered significant.

**2.8. siRNA Transfection.** Tumor cells were transfected with  $100 \mu\text{l}$  transfection mix ( $12 \mu\text{l}$  HiPerFect, Qiagen, Hilden, Germany,  $2.5 \mu\text{l}$  siRNA ( $20 \mu\text{M}$ ), and  $85.5 \mu\text{l}$  RPMI medium). siRNAs used were Hs\_PHF6\_10, SI05120745 and Hs\_PHF6\_11, SI05120752; Hs\_CD81\_6, SI02777236 and Hs\_CD81\_7, SI02777243; Hs\_CBX-3\_6, SI02665222 and Hs\_CBX-3\_7, SI03028165; and Hs\_ENSA\_20, SI05062218 and Hs\_

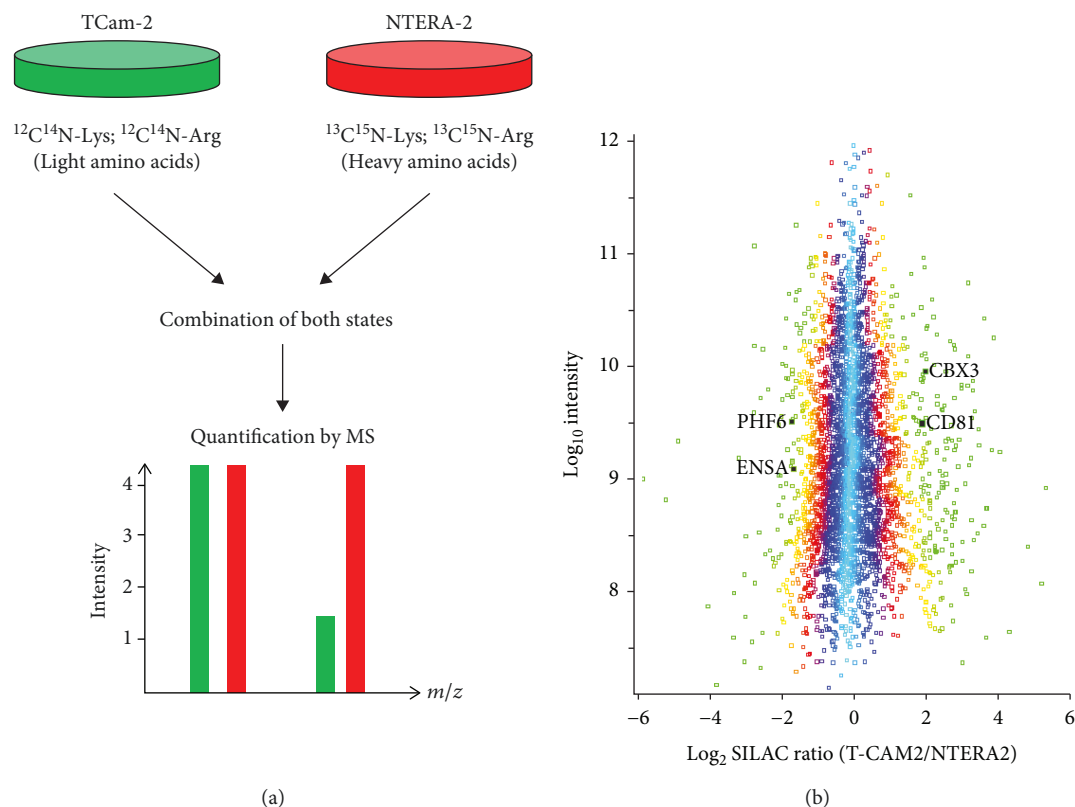


FIGURE 1: Proteomic profiling of testicular germ cell cancer cell lines. Workflow of SILAC-based mass spectrometry experiments. TCam-2 and NTERA-2 were metabolically labeled with amino acids of different masses allowing a comprehensive relative quantification of protein expression by mass spectrometry (a). Distribution of SILAC ratios of all quantified proteins according to their relative expression in NTERA-2 and TCam-2 (b).

ENSA\_21, SI05062225 (Qiagen, Hilden, Germany). After incubation for 20 min, 100  $\mu$ l siRNA medium were mixed with 2.3 ml culture medium to create a concentration of 1 : 1000. The cells were incubated for 24 h or 48 h.

**2.9. Measurement of Cell Proliferation.**  $1 \times 10^5$  to  $3 \times 10^5$  cells were plated as described above. After 48 h incubation time, the culture medium was exchanged for a siRNA medium (2.3 ml culture medium, 100  $\mu$ l siRNA-Mix). For cell viability analysis, equal numbers of cells were seeded into 96-well flat-bottom plates and incubated for indicated time points. Cell viability was determined by the CellTiter 96 AQueous One Solution Cell Proliferation Assay (MTS) (Promega) according to the manufacturer's instructions.

### 3. Results

**3.1. Quantitative Proteomic Profiling of TCam-2 and NTERA-2.** In order to find differences in the global proteome of seminoma-like and embryonal carcinoma-like cell lines, we performed a quantitative protein expression analysis by SILAC-based mass spectrometry. The cell lines TCam-2 (representing cell line with seminoma characteristics) and NTERA-2 (representing a cell line with embryonal carcinoma characteristics) were cultured with light and heavy isotope-labeled amino acids as described in the Material and Methods. After cell lysis, equal amounts of protein of

light-labeled TCam-2 were mixed with heavy-labeled NTERA-2 and vice versa and subsequently analyzed by high-resolution mass spectrometry. Due to the incorporation of SILAC amino acids, proteins derived from both cell lines can be accurately assigned to the two cell lines and its expression and can be comparatively quantified (Figure 1(a)). In two biological replicates, a total of 4856 proteins were identified and 3936 proteins could be quantified with a Gaussian distribution of the ratios between the two cell lines (Figure 1(b)). Next, an outlier significance score depending on intensity values (significance  $B$  in Perseus, see citation for more details [20, 21]) was calculated for every protein. 347 proteins showed a significantly different expression and 196 (TCam-2) and 102 (NTERA-2) proteins showed an at least 2.5-fold increased expression. The complete list of identified proteins detected by the quantitative MS is given in supplementary table 1, and the complete list of differentially expressed proteins is given in supplementary table 2.

**3.2. Bioinformatics Analysis Reveals Differential Pathway Activation Patterns.** The proteins showing significantly differential expression based on the results of the quantitative proteomic approach were subjected to a GO term analysis by the Metacore software (<https://portal.genego.com/>). The regulated proteins were found to be involved in different biological processes such as the regulation of tissue development or ion transport.



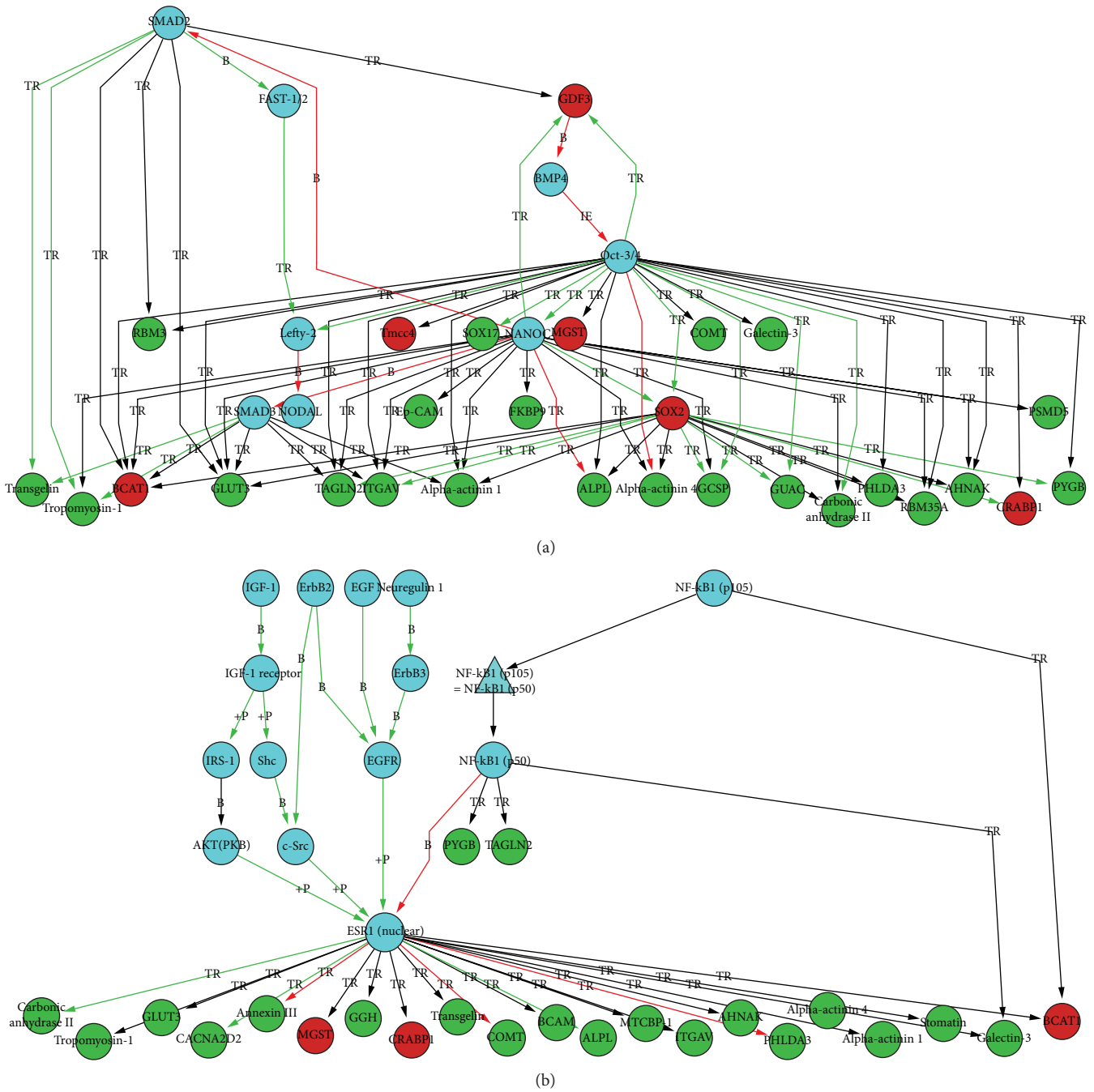


FIGURE 2: Results of network analysis: differentially regulated proteins from the SILAC approach are indicated in green (TCam-2) or in red (NTERA-2). Blue proteins represent proteins that were added from the Metacore database as potentially linked to the proteins from the SILAC analysis which are involved e.g. in gastrulation, endoderm development or formation of primary germ layer (a) and which are involved, e.g., in mammary gland development or fibroblast growth factor receptor signaling pathway (b). TR: transcription regulation; +P: phosphorylation; B: binding.

Network analysis was also performed using the Meta-core (<https://portal.genego.com/>) software for the enrichment of the shortest pathways inside the groups of differentially regulated proteins, as described above. Supplementary table 3 gives an overview of the networks found to be the most significantly involved. Inside the networks, differentially regulated proteins identified by the MS approach are indicated in green for TCam-2 (representing

seminomatous histology) or in red for NTERA-2 (representing nonseminomatous histology). Blue proteins represent proteins that were added from the Metacore database as potentially linked to the proteins derived from the MS analysis which are involved in different processes such as proteins which play a crucial role, for example, in gastrulation, endoderm development, or formation of a primary germ layer (Figure 2(a)) or mammary gland



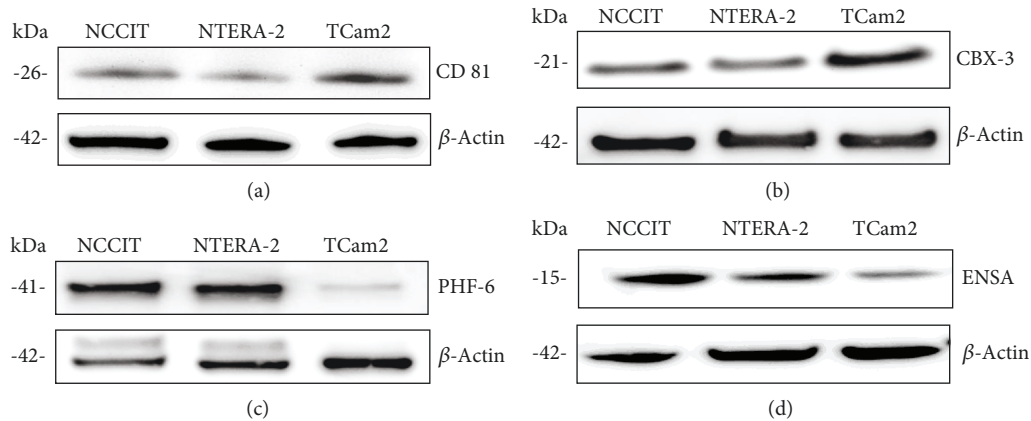


FIGURE 3: In vitro validation of differentially expressed proteins. In line with the results of the SILAC method and mass spectrometry, CD81 and CBX-3 show markedly higher expression in TCam-2 than in NTERA-2 (a, b). Conversely, PHF-6 and ENSA show markedly higher expression in NTERA-2 than in TCam-2 cells (c, d).

development or fibroblast growth factor receptor signaling pathway (Figure 2(b)).

**3.3. In Vitro and In Vivo Validation of Differentially Expressed Proteins.** To validate the results of the proteomics approach, four proteins were selected showing significant differences in expression between the two GCT-cell lines and which showed a physiological expression in nonneoplastic germ cells or several stages of spermatogenesis (according to The Human Protein Atlas database [17]), namely, CD81, CBX-3, PHF-6, and ENSA. In order to verify the differential protein expression, we additionally examined a third cell line named NCCIT (showing EC characteristics also).

Western blot analyses confirmed the results of the quantitative proteomic profiling. According to MS, the amount of CD81 (ratio  $TCam - 2/NTERA - 2 = 3.625$ ) and CBX-3 (ratio  $TCam - 2/NTERA - 2 = 3.281$ ) protein was significantly higher in TCam-2 than in NTERA-2- cells (supplementary table 2). These differences could be reproduced by western blot analysis for CD81 and CBX-3 which showed a marked difference in expression between the two cell lines with embryonal carcinoma characteristics (NTERA-2- and NCCIT) and TCam-2 (seminoma characteristics) (Figures 3(a) and 3(b)). In contrast, expression of PHF6 (ratio  $NTERA - 2/TCam - 2 = 3.841$ ) and ENSA (ratio  $NTERA - 2/TCam - 2 = 2.707$ ) proteins was significantly higher in NTERA-2 than in TCam-2 cells (supplementary table 2). These differences could also be reproduced by western blot analysis for PHF6 and ENSA, which showed marked differences in protein expression in NTERA-2 and NCCIT compared to TCam-2 (Figures 3(c) and 3(d)). The results confirmed the same expression pattern of NCCIT- and NTERA-2 cells in contrast to TCam-2 cells.

To confirm the results of the western blot analyses and gain insight into expression patterns within single cells of primary tumors (i.e., nuclear, cytoplasmic, or membranous staining), commercially available antibodies against CD81, CBX-3, PHF-6, and ENSA were used for immunohistochemical analysis of human tissues. FFPE tissue samples of 59 patients with malignant GCT of the testis were investigated

by immunohistochemical analysis. The investigated samples comprised tumor-free testicular tissue ( $n = 16$ ), GCNIS ( $n = 18$ ), seminomas ( $n = 21$ ), and embryonal carcinomas ( $n = 20$ ). Seminomas (to compare with TCam-2 cells) and embryonal carcinomas (to be compared with NTERA-2 and NCCIT cells) were explicitly chosen for direct a comparison with the cell lines.

A tumor-free testis showed a strong membranous and cytoplasmic expression of CD81 protein (Figure 4(a), arrow). In germ cell neoplasia *in situ* (GCNIS), a similar pattern of membranous and cytoplasmic expression was found (Figure 4(b), arrow). All investigated seminomas showed a strong membranous expression of CD81 in tumor cells (Figure 4(c), arrow). In contrast, no or only a weak staining of CD81 was seen in embryonal carcinoma cells (Figure 4(d), arrow). The differences in staining intensity (according to the immunoreactivity staining score (IRS)) of CD81 (Figure 4(e)) observed between seminomas and embryonal carcinomas were marked and showed a statistical significance.

CBX-3 protein showed a strong nuclear expression in spermatogonia, in contrast to a weaker expression in spermatocytes and spermatids (Figure 4(f), arrow). In addition, a strong nuclear expression of CBX-3 was observed in GCNIS (Figure 4(g), arrow). A strong nuclear expression was also detected in most seminoma cells (Figure 4(h), arrow). A much weaker nuclear expression of CBX-3 was seen in embryonal carcinomas (Figure 4(i), arrow). The differences in staining intensity (according to the immunoreactivity staining score (IRS)) of CBX-3 (Figure 4(j)) observed between seminomas and embryonal carcinomas were marked and showed a statistical significance. The results of CD81 and CBX-3 immunohistochemistry confirmed the findings of the proteomic and western blot analyses.

Immunohistochemically, PHF-6 protein showed strong nuclear expression in spermatogonia and slightly weaker expression in sertoli cells, whereas later stages of spermatogenesis did not express PHF-6 (Figure 5(a), arrow). The expression of PHF-6 in GCNIS was heterogeneous, with some nuclei showing strong and others weak or no expression (Figure 5(b), arrow). Seminomas showed no or

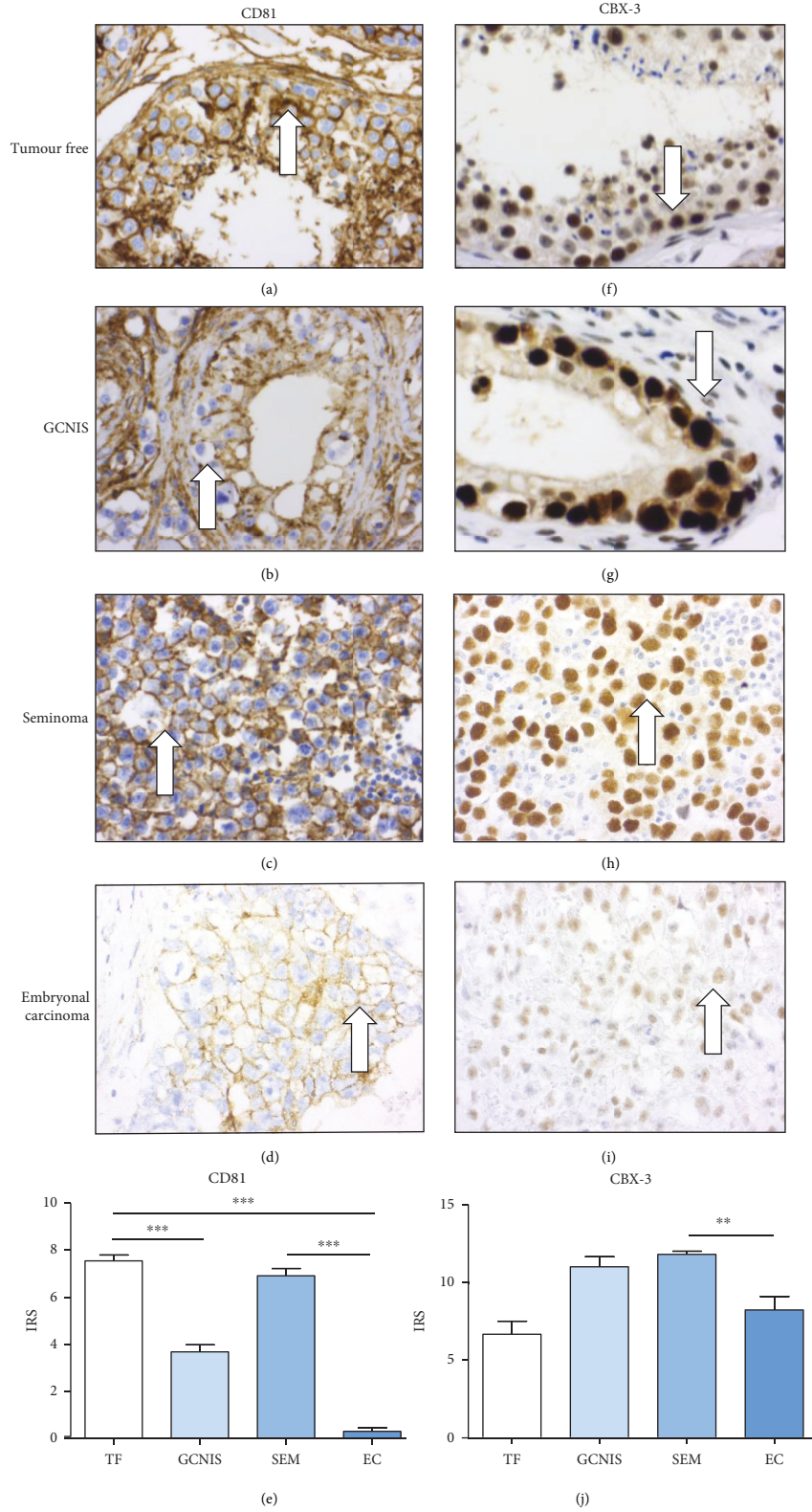


FIGURE 4: Immunohistochemical analysis of selected proteins (more highly expressed in TCam-2 than in NTERA-2) in tumor-free testis, GCNIS, seminoma, and embryonal carcinoma: a tumor-free testis and GCNIS show no differences in CD81 and CBX-3 >expression (a, b, f, g). The expression of CD81 and CBX-3 in embryonal carcinomas (d, i) is significantly lower than that in seminomas (c, h). The differences between seminomas and embryonal carcinomas in staining intensity (IRS) of CD81 (i) and CBX-3 (j) are significant.

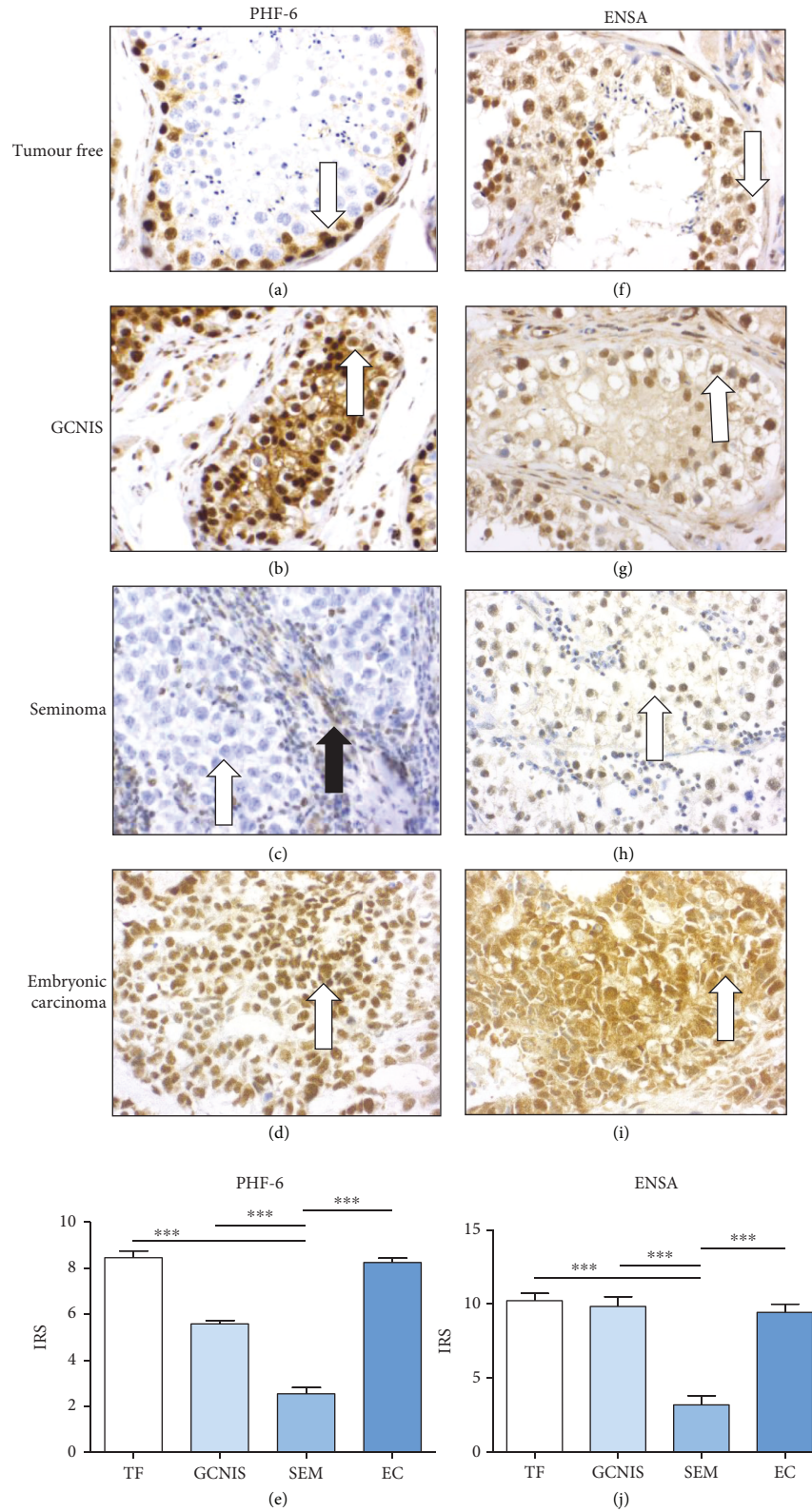


FIGURE 5: Immunohistochemical expression of selected proteins (more highly expressed in NTERA-2 than in TCam-2) in a tumor-free testis, GCNIS, seminoma, and embryonic carcinoma: A tumor-free testis and GCNIS show no marked differences in protein expression of PHF-6 and ENSA on immunohistochemical analysis (a, b, f, g). The expression of PHF-6 and ENSA in embryonic carcinomas (d, i) is markedly higher than that in seminomas (c, h; white arrow tumor cells, black arrow lymphocytes). The differences between seminomas and embryonic carcinomas in staining intensity (IRS) of PHF-6 (e) and ENSA (j) are significant.



only minimal expression of PHF-6 protein. Beside the tumor cells, lymphocytes also expressed PHF-6 (Figure 5(c), arrows). In contrast, embryonal carcinoma cells showed a strong nuclear expression of PHF-6 (Figure 5(d), arrow). The differences in staining intensity (according to the immunoreactivity staining score (IRS)) of PHF-6 (Figure 5(e)) observed between embryonal carcinomas and seminomas were marked and showed a statistical significance.

ENSA showed a strong nuclear and weak cytoplasmic expression in late stages of spermatogenesis, whereas spermatogonia were only weakly positive for ENSA (Figure 5(f), arrow). In addition, ENSA was found to be strongly expressed in GCNIS, mostly nuclear (Figure 5(g), arrow). Seminoma cells showed only a moderate nuclear expression of ENSA (Figure 5(h), arrow). Interestingly, nuclear as well as cytoplasmic expression of ENSA in embryonal carcinomas was significantly stronger than that in seminomas (Figure 5(i), arrow).

The differences in staining intensity (according to the immunoreactivity staining score (IRS)) of ENSA (Figure 5(j)) observed between embryonal carcinomas and seminomas were marked and showed a statistical significance. The results of PHF-6- and ENSA-immunohistochemistry confirmed the proteomic and western blot findings.

**3.4. Knockdown of Selected Proteins Results in Reduction of Cellular Survival in Seminoma and EC Cell Lines.** To gain insight into involved cellular processes and the putative role of selected proteins detected by MS, siRNA experiments were performed. The tumor cell lines NCCIT, NTERA-2, and TCam-2 were transfected with two specific siRNAs to achieve knockdown of CD81, CBX-3, PHF-6, and ENSA as described above. A marked downregulation of protein expression was achieved for all proteins for both siRNAs used (Figures 6(a)–6(d)).

This downregulation had no effect on proliferation after 24h (data not shown). 48h after downregulation of CD81, we observed a significant decrease of proliferation in NTERA-2, NCCIT, and TCam-2 cells. In NCCIT and NTERA-2, transfection with siRNA2 showed no statistical significances in proliferation (Figures 7(a)–7(c)). After the downregulation of CBX-3, we also observed a significant decrease of proliferation in all investigated GCT cell lines. SiRNA2 showed no statistical significances in proliferation in NTERA-2 cells (Figures 7(a)–7(c)). After the downregulation of PHF-6, we observed a significant decrease of proliferation in all investigated GCT cell lines, too. SiRNA2 had no effect in proliferation in TCam-2 cells (Figures 7(a)–7(c)). Finally, we observed a significant decrease of proliferation in all investigated GCT cell lines after downregulation of ENSA. SiRNA2 showed no statistical significances in proliferation in NCCIT cells (Figures 7(a)–7(c)). The decrease in proliferation after siRNA transfection appears to be independent of the different levels of expression of the proteins, as one might suspect.

## 4. Discussion

GCTs are highly interesting tumors, both from a point of view of developmental biology and considering their tumor

biology. GCTs are divided into seminomas and nonseminomas [2]. For *in vitro* studies, several GCT cell lines are well established, such as TCam-2 (with seminoma characteristics), NTERA-2, and NCCIT (both with characteristics of embryonal carcinomas) [7, 8, 22, 23]. We aimed to identify new biomarkers for the differentiation of GCT cell lines on the protein level. A recent study by van der Zwan et al. identified epigenetic footprints in TCam-2 and NCCIT cell lines. These analyses confirmed a more germ cell-like profile in TCam-2 cells and, in contrast, a more pluripotent phenotype in NCCIT cells [9]. We compared the results of a differential gene expression in TCam-2 and NCCIT cells of the work by van der Zwan et al. [9] to the results of our project and found 44 (TCam-2) and 23 (NTERA-2 or NCCIT) similarly significantly differentially expressed proteins/genes. The exact names of the genes are listed in Table 1. This underpins the potential importance of these genes in the biology of these tumor cells.

In addition, we searched for proteins that were differently expressed in cell lines and that are expressed physiologically in spermatogonia and later stages of spermatogenesis. Furthermore, we analyzed if the findings from the cell line experiments were reproducible in FFPE tissue samples of human GCTs. In the present study, 111 proteins showed a statistically significant two-fold increase in expression in TCam-2 compared to NTERA-2. Influenced by the expression pattern in spermatogenesis and germ cell tumors (according to The Human Protein Atlas database [17]) by the availability of antibodies and their applicability on both, cell lines and FFPE tissues, we chose the proteins CD81 (ratio from SILAC-analysis TCam-2/NTERA-2: 3.626) and CBX-3 (ratio TCam-2/NTERA-2: 3.282) for further investigations.

CD81 is a cell surface protein of the tetraspanin family. It is widely expressed on many healthy tissues and on the majority of tumor cells. Vences-Catalan et al. demonstrated in comprehensive studies the role of CD81 as a promoter of tumor growth and metastasis with a putatively important role in tumor progression [24, 25]. Zhang et al. described that an increased expression of CD81 was significantly associated with reduced overall survival in patients with mammary carcinoma. Furthermore, CD81 knockdown results in decreased proliferation and migration in mammary carcinoma cell lines *in vitro* [26]. In addition, Hong et al. described that CD81 increases melanoma cell motility by upregulating the metalloproteinase MT1-MMP-expression. This could be explained by a prooncogenic Akt-dependent Sp1 activation [27]. Interestingly, in our study, we could demonstrate that CD81 showed marked differences in its expression when comparing seminoma (high expression) and embryonal carcinoma tissue samples (low expression). CD81 interacts with CD9 (another member of the tetraspanin family), which is also significantly upregulated in TCam-2 cells (supplementary table 2), and both play an important role in the TGF beta signaling pathway in melanoma cells [28]. TGF beta, EGF, and FGF have been shown to play a role in the differentiation of TCam-2 into a cell type resembling a mixed nonseminoma [7]. This would be in line with the findings of our study, as shown in Figure 2, where involved

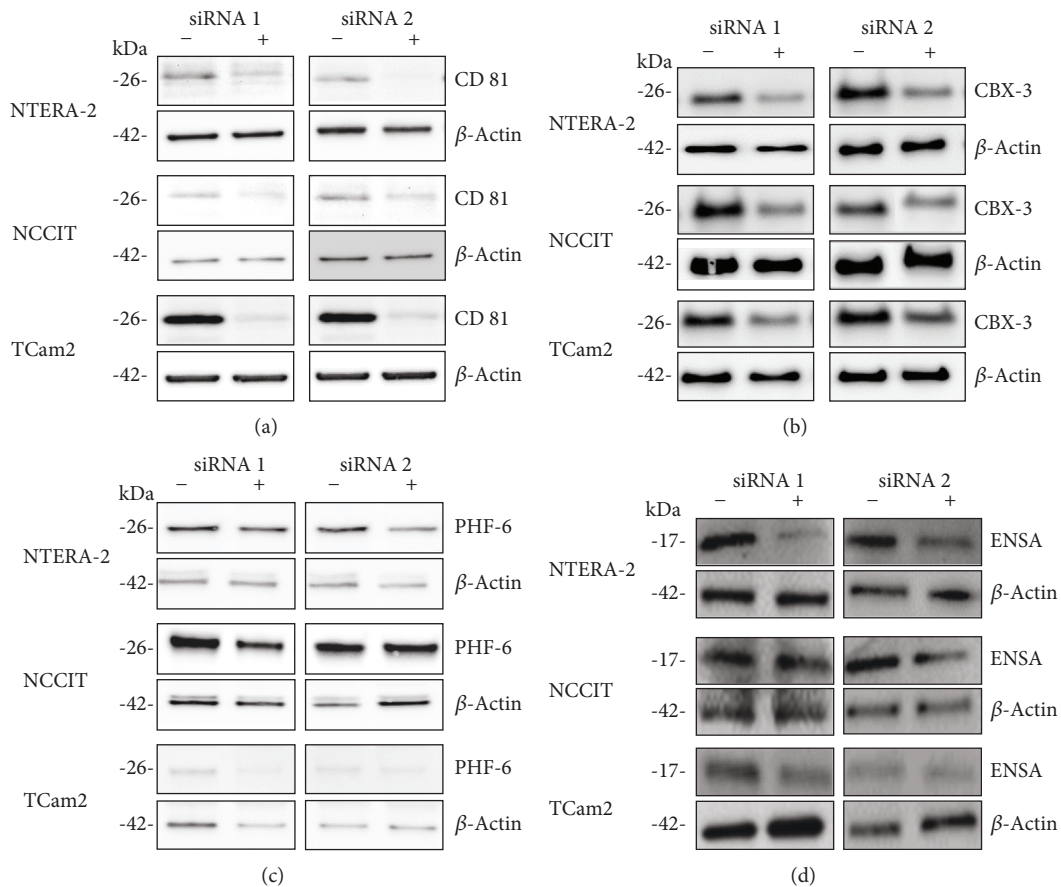


FIGURE 6: Transfection with siRNA markedly reduces protein expression of CD81, CBX-3, PHF-6, and ENSA: NCCIT, NTERA-2, and TCam-2 were transfected with a siRNAs against CD81, CBX-3, PHF-6, and ENSA. The protein expression was markedly reduced after transfection with siRNA (a–d).

networks are displayed and demonstrate that these growth factor signaling pathways play a crucial role. In addition, first investigations with two siRNAs against CD81 showed a significant reduction of proliferation in TCam-2 cells, as well as in NTERA-2 and NCCIT cells (Figure 7). So the extent of proliferation seems not to correlate with the expression level of CD81. Usually, TCam-2 cells proliferate remarkably slower than NTERA-2 and NCCIT. However, the high expression of CD81 on TCam-2 and seminoma samples is interesting given the induction of nonseminoma-like phenotype by TGF beta signaling [6]. However, the exact mechanism on how the proliferation was reduced in this cell line has not been investigated in more detail and remains to be elucidated.

A second protein which was markedly higher expressed in TCam-2 cells than in NTERA-2 and NCCIT cells is CBX-3. Little is known about the function of CBX-3 in cancer cells. One study could demonstrate the essential function of CBX-3 for male germ cell survival and spermatogenesis [29]. Ma et al. described very recently that the expression of CBX-3 in osteosarcomas is associated with a large tumor size, high distant metastasis rate, and high clinical stage rate. Furthermore, they could show that knockdown of CBX-3 by siRNA results in increased apoptosis and cell cycle arrest at the G0 and G1 phases [30]. Another recent study

demonstrates the role of CBX-3 in tumor progression in pancreatic cancer cell lines. It could be shown that the tumor-promoting effect of CBX-3 might be mediated by CDK1 [31]. Further similar results were demonstrated by Zhang et al. which demonstrate that a high expression of CBX-3 in squamous carcinomas of the tongue is associated with poor prognosis. In addition, the inhibition of CBX-3 leads to cell cycle delay via the p21 pathway [32]. Similar findings were described by Fan et al. who showed that CBX-3 promotes the progression of the cell cycle and proliferation *in vitro* and *in vivo* in colon cancer cells. They could explain that CBX-3 promotes colon cancer cell proliferation by curbing cell cycle G1-S phase transition [33]. Another study showed a high expression of CBX-3 in various human cancer tissues and suppression of tumor growth of various cancer-derived cell lines following siRNA-mediated knockdown [34]. Again, we found that two siCBX-3 reduced tumor cell growth in all investigated GCT cell lines. Further investigations of the mechanisms underlying this observation and a potential role in antitumor therapy are pending.

Our investigations furthermore showed markedly higher expression of PHF-6 in NTERA-2 and NCCIT cell lines as compared to TCam-2. PHF-6 is a gene found in association with the *Börjeson-Forssman-Lehmann syndrome*



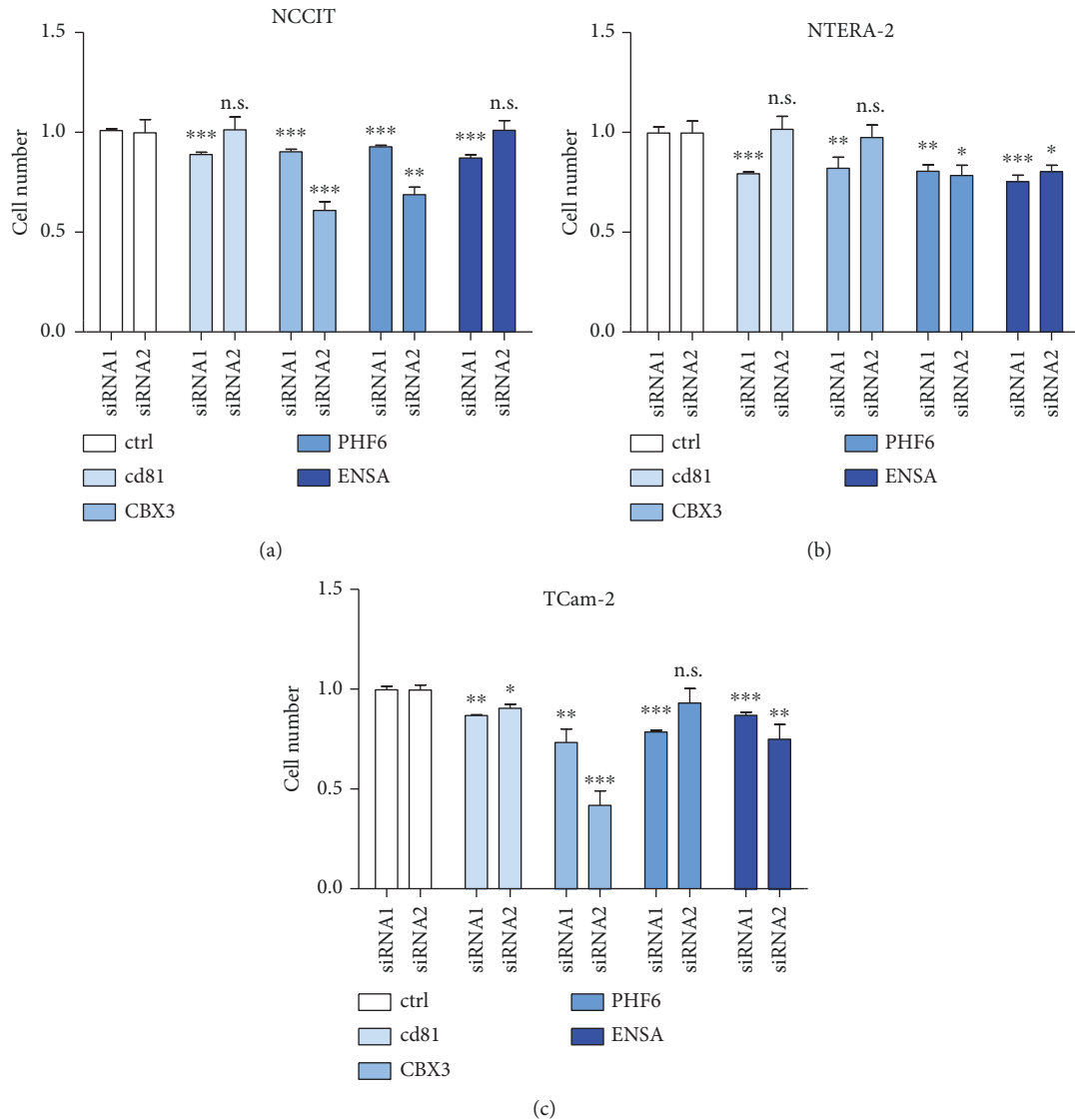


FIGURE 7: Transfection with siRNA decreases cell proliferation of GCT cell lines: in all investigated tumor cell lines, NCCIT (a), NTERA-2 (b), and TCam-2 (c), proliferation was significantly reduced after transfection with siRNA against CD81, CBX-3, PHF-6, and ENSA.

[35]. Interestingly, patients with this syndrome generally show hypogonadism [36]. Our results show a strong nuclear positivity of the PHF-6 protein in normal spermatogenesis and GCNIS, whereas the expression in seminomas was markedly lower. Notably, PHF-6 expression was markedly higher in embryonal carcinomas, than in seminomas in FFPE samples. Recently, PHF-6 has been described to be involved in regulating rRNA synthesis, which may contribute to its role in cell cycle control, maintenance of genomic integrity, and tumor suppression [37]. This would be in line with our results which show that siPHF-6 suppresses cell proliferation in GCT cell lines (Figure 7).

Finally, ENSA (alpha-endosulfine) is a potent inhibitor of PP2A-B55 $\delta$  [38, 39]. PP2A is expressed in both primary GCTs and GCT cell lines. Its inhibition mediates an apoptosis induction in GCT cells through activation of the MEK-ERK signaling pathway [40]. Furthermore, inhibition of ENSA with two specific siRNAs leads to reduced cell prolifer-

ation in all investigated GCT cell lines. Seminoma cells showed only a moderate nuclear expression (Figure 5(h)), in contrast to embryonal carcinomas which show a significantly stronger expression of ENSA than seminomas. However, this finding supports the close developmental relationship between early spermatogenesis and seminomas in contrast to embryonal carcinomas.

Using network analysis, the differently expressed proteins identified by our proteomic analysis could be linked to the proteins assigned from the Metacore database. Proteins were closely linked to proteins such as SOX-2, SOX-17, NANOG, or OCT3/4, which all have been described to play crucial roles in pluripotency and differentiation of germ cells and germ cell tumors [41–43]. Interestingly, another putative stem cell gene, GDF-3, has been found to be expressed in both seminomas and breast carcinomas [42]. The increased expression of BCAT1 in NTERA-2 cells compared to TCam-2 cells seems also of interest in distinguishing germ

TABLE 1: Differentially expressed genes compared with van der Zwan et al. [9] and the results of the present study. The table shows the identical genes, which are differentially expressed in NCCIT or NTERA-2 compared to TCam-2.

Increased in TCam-2	Increased in NTERA-2/NCCIT
ACSF2	ACAT2
ANXA1	AP1S2
ANXA3	ARMCX2
CACNA2D2	ARRB1
COL17A1	ASS1
COL23A1	BCAT1
COMT	CIQBP
CSRP1	CECR5
DUSP23	CRABP1
EFR3A	CTSC
ENO2	DPYSL3
EPCAM	GFPT2
FLNC	HPRT1
GLIPR2	IQGAP2
GMPR	MAD2L2
GSN	MGST1
HEG1	PFAS
HIC2	PNMA2
ITGAV	POLR3G
LAMA5	SH3BGRL
ODZ4	SOX2
PHLDA3	TMCO1
PPM1F	UGP2
PRAME	
PROM1	
PSD3	
PSTPIP2	
PVR	
PYGB	
RAB15	
RASSF2	
RCN1	
SDF2L1	
SERPINE2	
SLC25A29	
SPARC	
TAGLN	
TCL1A	
TFAP2C	
TMEM132A	
VAMP8	
VSNL1	
WASL	

cell tumor subtypes. These findings are in line with the results of Rodriguez et al., which could demonstrate a strong overexpression of BCAT-1 in nonseminomas germ cell tumors [44].

## 5. Conclusion

In summary, high-resolution mass spectrometry in combination with SILAC-quantification is suitable for the detection of differentially expressed proteins in GCT cell lines. These results could be reproduced by western blot analysis. Proteins detected as differentially expressed by SILAC-based MS could furthermore be validated in FFPE samples of human GCTs and normal (tumor-free) testes. This method is therefore valuable for the detection of new markers with the potential to distinguish between different histologic subtypes of these tumors. In addition, network analyses serve to classify the differentially expressed proteins into functional groups. Finally, siRNA results indicate an antiproliferative potential of the therapeutic knockdown of several detected proteins, which warrants their evaluation as potential therapeutic targets.

## Data Availability

We have submitted our raw and processed mass-spectrometry data to the PRIDE proteomics data repository (<http://www.ebi.ac.uk/pride/archive/>), to allow a thorough evaluation of the results (Project accession: PXD010275; Account details: reviewer33380@ebi.ac.uk; password: TrOAL2N5).

## Conflicts of Interest

The authors declare that they have no conflict of interest.

## Authors' Contributions

Felix Bremmer, Hanibal Bohnenberger, Stefan Balabanov, and Friedemann Honecker contributed equally to this work.

## Acknowledgments

F.B. is supported by the Wilhelm Sander-Stiftung (Grant numbers 2016.041.1 and 2016.041.2). H.B. is supported by the Deutsche Krebshilfe Foundation (grant 70112551), the University Medical Center Göttingen, and the Else Kröner-Fresenius-Stiftung. We thank Olga Dschun and Josephine Psotta for the perfect technical assistance. We acknowledge the support from the German Research Foundation and the Open Access Publication Funds of the Göttingen University.

## Supplementary Materials

*Supplementary 1.* Supplementary Table 1 Complete list of identified proteins detected by the quantitative mass spectrometry as revealed by MaxQuant analysis of the obtained MS raw data.

*Supplementary 2.* Supplementary Table 2 Differentially expressed proteins in TCam-2 and NTERA-2.

*Supplementary 3. Supplementary Table 3. Significantly involved networks of proteins detected by SILAC and mass spectrometry.*

## References

- [1] J. Beyer, P. Albers, R. Altena et al., "Maintaining success, reducing treatment burden, focusing on survivorship: highlights from the third European consensus conference on diagnosis and treatment of germ-cell cancer," *Annals of Oncology*, vol. 24, no. 4, pp. 878–888, 2013.
- [2] H. Moch, A. L. Cubilla, P. A. Humphrey, V. E. Reuter, and T. M. Ulbright, "The 2016 WHO classification of tumours of the urinary system and male genital organs-part a: renal, penile, and Testicular Tumours," *European Urology*, vol. 70, no. 1, pp. 93–105, 2016.
- [3] D. M. Berney, L. H. J. Looijenga, M. Idrees et al., "Germ cell neoplasia *in situ* (GCNIS): evolution of the current nomenclature for testicular pre-invasive germ cell malignancy," *Histopathology*, vol. 69, no. 1, pp. 7–10, 2016.
- [4] "International Germ Cell Consensus Classification: a prognostic factor-based staging system for metastatic germ cell cancers. International Germ Cell Cancer Collaborative Group," *Journal of Clinical Oncology*, vol. 15, no. 2, pp. 594–603, 1997.
- [5] C. Bokemeyer, K. Oechsle, F. Honecker et al., "Combination chemotherapy with gemcitabine, oxaliplatin, and paclitaxel in patients with cisplatin-refractory or multiply relapsed germ-cell tumors: a study of the German Testicular Cancer Study Group," *Annals of Oncology*, vol. 19, no. 3, pp. 448–453, 2007.
- [6] D. R. Feldman, G. J. Bosl, J. Sheinfeld, and R. J. Motzer, "Medical treatment of advanced testicular cancer," *Journal of the American Medical Association*, vol. 299, no. 6, pp. 672–684, 2008.
- [7] D. Nettersheim, A. J. M. Gillis, L. H. J. Looijenga, and H. Schorle, "TGF- $\beta$ 1, EGF and FGF4 synergistically induce differentiation of the seminoma cell line TCam-2 into a cell type resembling mixed non-seminoma," *International Journal of Andrology*, vol. 34, no. 4, Part2, pp. e189–e203, 2011.
- [8] R. Eini, H. Stoop, A. J. M. Gillis, K. Biermann, L. C. J. Dorssers, and L. H. J. Looijenga, "Role of SOX2 in the etiology of embryonal carcinoma, based on analysis of the NCCIT and NT2 cell lines," *PLoS One*, vol. 9, no. 1, article e83585, 2014.
- [9] Y. G. van der Zwan, M. A. Rijlaarsdam, F. J. Rossello et al., "Seminoma and embryonal carcinoma footprints identified by analysis of integrated genome-wide epigenetic and expression profiles of germ cell cancer cell lines," *PLoS One*, vol. 9, no. 6, article e98330, 2014.
- [10] B. Zhang, J. Wang, X. Wang et al., "Proteogenomic characterization of human colon and rectal cancer," *Nature*, vol. 513, no. 7518, pp. 382–387, 2014.
- [11] L. H. J. Looijenga, H. Stoop, and K. Biermann, "Testicular cancer: biology and biomarkers," *Virchows Archiv*, vol. 464, no. 3, pp. 301–313, 2014.
- [12] M. Bantscheff, M. Schirle, G. Sweetman, J. Rick, and B. Kuster, "Quantitative mass spectrometry in proteomics: a critical review," *Analytical and Bioanalytical Chemistry*, vol. 389, no. 4, pp. 1017–1031, 2007.
- [13] S. E. Ong, B. Blagoev, I. Kratchmarova et al., "Stable isotope labeling by amino acids in cell culture, SILAC, as a simple and accurate approach to expression proteomics," *Molecular & Cellular Proteomics*, vol. 1, no. 5, pp. 376–386, 2002.
- [14] H. Bohnenberger, L. Kaderali, P. Ströbel et al., "Comparative proteomics reveals a diagnostic signature for pulmonary head-and-neck cancer metastasis," *EMBO Molecular Medicine*, vol. 10, no. 9, article e8428, 2018.
- [15] H. Bohnenberger, T. Oellerich, M. Engelke, H. H. Hsiao, H. Urlaub, and J. Wienands, "Complex phosphorylation dynamics control the composition of the Syk interactome in B cells," *European Journal of Immunology*, vol. 41, no. 6, pp. 1550–1562, 2011.
- [16] T. Oellerich, V. Bremes, K. Neumann et al., "The B-cell antigen receptor signals through a preformed transducer module of SLP65 and CIN85," *Embo Journal*, vol. 30, no. 17, pp. 3620–3634, 2011.
- [17] M. Uhlen, L. Fagerberg, B. M. Hallstrom et al., "Tissue-based map of the human proteome," *Science*, vol. 347, no. 6220, article 1260419, 2015.
- [18] F. Bremmer, S. Schallenberg, H. Jarry et al., "Role of N-cadherin in proliferation, migration, and invasion of germ cell tumours," *Oncotarget*, vol. 6, no. 32, pp. 33426–33437, 2015.
- [19] F. Bremmer, S. Schweyer, M. Martin-Ortega et al., "Switch of cadherin expression as a diagnostic tool for Leydig cell tumours," *APMIS*, vol. 121, no. 10, pp. 976–981, 2013.
- [20] J. Cox and M. Mann, "MaxQuant enables high peptide identification rates, individualized p.p.b.-range mass accuracies and proteome-wide protein quantification," *Nature Biotechnology*, vol. 26, no. 12, pp. 1367–1372, 2008.
- [21] S. Tyanova, T. Temu, P. Sinitcyn et al., "The Perseus computational platform for comprehensive analysis of (prote)omics data," *Nature Methods*, vol. 13, no. 9, pp. 731–740, 2016.
- [22] J. de Jong, H. Stoop, A. J. M. Gillis et al., "Further characterization of the first seminoma cell line TCam-2," *Genes, Chromosomes and Cancer*, vol. 47, no. 3, pp. 185–196, 2008.
- [23] S. Teshima, Y. Shimosato, S. Hirohashi et al., "Four new human germ cell tumor cell lines," *Laboratory Investigation*, vol. 59, no. 3, pp. 328–336, 1988.
- [24] F. Vences-Catalán, R. Rajapaksa, M. K. Srivastava et al., "Tetraspanin CD81 promotes tumor growth and metastasis by modulating the functions of T regulatory and myeloid-derived suppressor cells," *Cancer Research*, vol. 75, no. 21, pp. 4517–4526, 2015.
- [25] F. Vences-Catalán, R. Rajapaksa, M. K. Srivastava et al., "Tetraspanin CD81, a modulator of immune suppression in cancer and metastasis," *Oncoimmunology*, vol. 5, no. 5, article e1120399, 2016.
- [26] N. Zhang, L. Zuo, H. Zheng, G. Li, and X. C. Hu, "Increased expression of CD81 in breast cancer tissue is associated with reduced patient prognosis and increased cell migration and proliferation in MDA-MB-231 and MDA-MB-435S human breast cancer cell lines *in vitro*," *Medical Science Monitor*, vol. 24, pp. 5739–5747, 2018.
- [27] I. K. Hong, H. J. Byun, J. Lee et al., "The tetraspanin CD81 protein increases melanoma cell motility by up-regulating metalloproteinase MT1-MMP expression through the oncogenic Akt-dependent Sp1 activation signaling pathways," *Journal of Biological Chemistry*, vol. 289, no. 22, pp. 15691–15704, 2014.

- [28] H. X. Wang and M. E. Hemler, "Novel impact of EWI-2, CD9, and CD81 on TGF- $\beta$  signaling in melanoma," *Molecular & Cellular Oncology*, vol. 2, no. 4, 2015.
- [29] J. P. Brown, J. Bullwinkel, B. Baron-Lühr et al., "HP1gamma function is required for male germ cell survival and spermatogenesis," *Epigenetics & Chromatin*, vol. 3, no. 1, p. 9, 2010.
- [30] C. Ma, X. G. Nie, Y. L. Wang et al., "CBX3 predicts an unfavorable prognosis and promotes tumorigenesis in osteosarcoma," *Molecular Medicine Reports*, vol. 19, no. 5, pp. 4205–4212, 2019.
- [31] L. Y. Chen, C. S. Cheng, C. Qu et al., "Overexpression of CBX3 in pancreatic adenocarcinoma promotes cell cycle transition-associated tumor progression," *International Journal of Molecular Sciences*, vol. 19, no. 6, p. 1768, 2018.
- [32] H. Y. Zhang, W. C. Chen, X. Y. Fu, X. Su, and A. K. Yang, "CBX3 promotes tumor proliferation by regulating G1/S phase via p21 downregulation and associates with poor prognosis in tongue squamous cell carcinoma," *Gene*, vol. 654, pp. 49–56, 2018.
- [33] Y. Fan, H. P. Li, X. L. Liang, and Z. Xiang, "CBX3 promotes colon cancer cell proliferation by CDK6 kinase-independent function during cell cycle," *Oncotarget*, vol. 8, no. 12, pp. 19934–19946, 2017.
- [34] M. Takanashi, K. Oikawa, K. Fujita, M. Kudo, M. Kinoshita, and M. Kuroda, "Heterochromatin protein 1 $\gamma$  epigenetically regulates cell differentiation and exhibits potential as a therapeutic target for various types of cancers," *The American Journal of Pathology*, vol. 174, no. 1, pp. 309–316, 2009.
- [35] A. Baumstark, K. M. Lower, A. Sinkus et al., "Novel PHF6 mutation p.D333del causes Borjeson-Forssman-Lehmann syndrome," *Journal of Medical Genetics*, vol. 40, no. 4, article e50, pp. 50e–550, 2003.
- [36] M. Borjeson, H. Forssman, and O. Lehmann, "An X-linked, recessively inherited syndrome characterized by grave mental deficiency, epilepsy, and endocrine disorder," *Acta Medica Scandinavica*, vol. 171, pp. 13–21, 1962.
- [37] J. Wang, J. W. Leung, Z. Gong, L. Feng, X. Shi, and J. Chen, "PHF6 regulates cell cycle progression by suppressing ribosomal RNA synthesis," *The Journal of Biological Chemistry*, vol. 288, no. 5, pp. 3174–3183, 2013.
- [38] A. Gharbi-Ayachi, J. C. Labbe, A. Burgess et al., "The substrate of Greatwall kinase, Arpp19, controls mitosis by inhibiting protein phosphatase 2A," *Science*, vol. 330, no. 6011, pp. 1673–1677, 2010.
- [39] S. Mochida, S. L. Maslen, M. Skehel, and T. Hunt, "Greatwall phosphorylates an inhibitor of protein phosphatase 2A that is essential for mitosis," *Science*, vol. 330, no. 6011, pp. 1670–1673, 2010.
- [40] S. Schwyer, A. Bachem, F. Bremmer et al., "Expression and function of protein phosphatase PP2A in malignant testicular germ cell tumours," *The Journal of pathology*, vol. 213, no. 1, pp. 72–81, 2007.
- [41] J. de Jong, H. Stoop, A. J. M. Gillis et al., "Differential expression of SOX17 and SOX2 in germ cells and stem cells has biological and clinical implications," *The Journal of Pathology*, vol. 215, no. 1, pp. 21–30, 2008.
- [42] U. I. Ezech, P. J. Turek, R. A. Reijo, and A. T. Clark, "Human embryonic stem cell genes *OCT4*, *NANOG*, *STELLAR*, and *GDF3* are expressed in both seminoma and breast carcinoma," *Cancer*, vol. 104, no. 10, pp. 2255–2265, 2005.
- [43] A. H. Hart, L. Hartley, K. Parker et al., "The pluripotency homeobox gene *NANOG* is expressed in human germ cell tumors," *Cancer*, vol. 104, no. 10, pp. 2092–2098, 2005.
- [44] S. Rodriguez, O. Jafer, H. Goker et al., "Expression profile of genes from 12p in testicular germ cell tumors of adolescents and adults associated with i(12p) and amplification at 12p11.2-p12.1," *Oncogene*, vol. 22, no. 12, pp. 1880–1891, 2003.

## Research Article

# De Ritis Ratio (Aspartate Transaminase/Alanine Transaminase) as a Significant Prognostic Factor in Patients Undergoing Radical Cystectomy with Bladder Urothelial Carcinoma: A Propensity Score-Matched Study

Hyeong Dong Yuk <sup>1</sup>, Chang Wook Jeong,<sup>2</sup> Cheol Kwak,<sup>2</sup> Hyeon Hoe Kim,<sup>2</sup> and Ja Hyeon Ku <sup>2</sup>

<sup>1</sup>Department of Urology, Inje University Sanggye Paik Hospital, Seoul, Republic of Korea

<sup>2</sup>Department of Urology, Seoul National University Hospital, Seoul, Republic of Korea

Correspondence should be addressed to Ja Hyeon Ku; [randyku@hanmail.net](mailto:randyku@hanmail.net)

Received 4 June 2019; Accepted 7 August 2019; Published 27 August 2019

Guest Editor: Giovanni Cochetti

Copyright © 2019 Hyeong Dong Yuk et al. This is an open access article distributed under the Creative Commons Attribution License, which permits unrestricted use, distribution, and reproduction in any medium, provided the original work is properly cited.

**Introduction.** To investigate the correlation between preoperative De Ritis ratio (aspartate transaminase (AST)/alanine transaminase (ALT)) and postoperative outcome in patients with urothelial cell carcinoma (UC) treated with radical cystectomy. **Materials and Methods.** We analyzed the clinical and pathological data of 771 patients who underwent radical cystectomy for bladder UC. Patients were divided into two groups according to the optimal value of AST/ALT ratio. The effect of the AST/ALT ratio was analyzed using the Kaplan–Meier method and Cox regression hazard models for patients' cancer-specific survival (CSS), overall survival (OS), and recurrence-free survival (RFS). In addition, propensity score matching of 1 : 1 was performed between the two groups. **Results.** Median follow-up was 84.0 (36–275) months. Mean age was  $64.8 \pm 10.0$  years. According to the receiver operating characteristic (ROC) analysis, the optimal threshold of the AST/ALT ratio was 1.1. In Kaplan–Meier analyses, the high AST/ALT group showed worse outcomes in CSS and OS (all  $P < 0.001$ ). Also, RFS ( $P = 0.001$ ) in the Cox regression models of clinical and pathological parameters was used to predict CSS, OS, and AST/ALT ratio (HR 2.15, 95% CI 1.23–3.73,  $P = 0.007$ ) and pathological T stage (HR 4.80, 95% CI 1.19–19.28,  $P = 0.003$ ). To predict OS and AST/ALT ratio (HR 2.05, 95% CI 1.65–2.56,  $P < 0.001$ ), pathological T stage (HR 2.96, 95% CI 0.57–17.09,  $P = 0.037$ ) and positive lymph node (HR 1.71, 95% CI 1.50–1.91,  $P = 0.021$ ) were determined as independent prognostic factors. **Conclusion.** Preoperative AST/ALT ratio could be an independent prognostic factor in patients with UC treated with radical cystectomy.

## 1. Introduction

Bladder cancer is a common cancer in the urinary tract [1] and is the ninth most common cancer worldwide [2]. The most common histopathological type of bladder cancer is urothelial cell carcinoma (UC). In bladder UC diagnosis, 75% of cases are diagnosed as nonmuscle invasive bladder cancer (NMIBC) and 25% are diagnosed as muscle invasive bladder cancer (MIBC) at the time of diagnosis [3–5]. Radical cystectomy is the standard treatment for

the highest risk of NMIBC progression and high-risk NMIBC intolerant to intravesical treatment and localized or regionally advanced MIBC [4–6]. However, even if radical cystectomy is performed, the prognosis is poor. Recurrence occurs in more than 30% of patients after radical cystectomy [7], and bladder cancer is the 13th most common cause of cancer deaths [2].

Various biomarkers have been discussed for early diagnosis and prognosis prediction of bladder cancer [8, 9], such as nuclear matrix protein 22, bladder tumor antigen, soluble



FAS, fibroblast growth factor receptor 3, methylation biomarkers, and cytokeratin 20 [8]. In addition, there are several mRNA-based biomarker tests such as Cxbladder monitor, XPERT BC, and bladder cancer test [9].

Alanine aminotransferase (ALT) and aspartate aminotransferase (AST) are well-known liver enzymes found in the heart, skeletal muscle, brain, kidney, and red blood cells, in addition to the liver. Because of this characteristic, they are also used as an indicator of other diseases [10, 11]. These enzymes are used as biomarkers that can predict prognosis in several malignancies such as lung, colorectal, pancreas, breast, and kidney [12–16]. Serum ratios of AST and ALT as well as AST and ALT have also been reported to play a role as biomarkers. De Ritis first reported on the serum activity ratio of AST and ALT as an assessment tool for disease in viral hepatitis studies [17]. AST/ALT ratio has also been reported in recent years as a biomarker that can predict prognosis in renal cell carcinoma [18]. It was reported that AST/ALT might be associated with anaerobic glycolysis [19]. This glucose metabolism was also reported to be associated with urothelial carcinoma (UC), and the association of AST/ALT ratio with the prognosis was reported in upper tract urothelial carcinoma (UTUC) [20]. Therefore, the aim of this study was to evaluate the prognostic value of AST/ALT in UC of the bladder in patients with radical cystectomy.

## 2. Materials and Methods

**2.1. Study Sample.** We retrospectively reviewed the medical records of patients who underwent radical cystectomy for bladder urothelial cell cancer at Seoul National University Hospital from 1991 to 2015. T2-T4 or intravesical bacillus Calmette-Guerin (BCG) intolerance T1 high-grade. All patients underwent radical cystectomy with pelvic lymph node dissection. Patients with a short follow-up period of less than 2 years were excluded. Patients with preoperative liver disease, infection, leukocytosis, inflammatory condition, and muscle-related disease were excluded. Six hundred and seventy-one patients were included. The study was approved by the institutional ethical review board (approval code: H-1903-133-1020), and the study protocol and all related content adhered to the guidelines of the Helsinki declaration.

**2.2. Study Design.** Patients were divided into two groups according to the optimal value of the AST/ALT ratio. The optimal value of the AST/ALT ratio was obtained using the receiver operating characteristic (ROC) curve with the highest sensitivity and specificity. The optimum value of AST/ALT thus obtained was 1.1. Patients were divided into two groups based on AST/ALT 1.1. Clinical and pathological information and prognosis of the two groups were compared. In addition, 1:1 propensity matching was performed to compensate for the difference between age, sex, BMI, ASA, neoadjuvant chemotherapy, operative type, and diversion type. The patient's clinical and pathological information was reviewed. Clinical and pathological information included age, gender, body mass index (BMI), American Society of Anesthesiologists (ASA) physical status, operative method,

urinary diversion type, pathological tumor/lymph nodes/metastasis (TNM) staging, presence of margin positive, carcinoma in situ, lymphovascular invasion (LVI), number of removed lymph nodes, number of positive lymph nodes, neoadjuvant and adjuvant chemotherapy, and adjuvant radiotherapy. Oncologic outcomes data were also collected for recurrence, mortality, and mortality due to cancer.

All patients were admitted to the hospital 2 days before surgery to undergo a 2-day bowel preparation. A preoperative laboratory blood test was performed at admission. Postoperative follow-up was performed according to our hospital protocol as follows. Follow-up was performed every 3 months until 3 years after radical cystectomy, every 6 months for 5 years postoperative, and every year after the first 5 years postoperative. Routine laboratory tests, urine cytology, urine analysis, and cystoscopy were performed at each follow-up after radical cystectomy. In addition, ultrasonography bladder scans for a postvoid urine check were performed at each follow-up in neobladder patients. Computed tomography (CT) and bone scans were performed every year [21].

**2.3. Statistical Analysis.** The analysis of the continuous variables was expressed as a median value and interquartile range (IQR) or mean value and standard deviation (SD) using descriptive statistics. The analysis of nominal variables is expressed as probability (%) using crossover analysis. The primary endpoint was overall survival (OS), and the secondary endpoints were recurrence-free survival (RFS) and cancer-specific survival (CSS). All oncologic outcomes were analyzed using Kaplan–Meier survival analysis and logrank test. Various factors affecting oncologic outcome were analyzed using Cox proportional hazard regression analysis. Additionally, 1:1 propensity score matching was performed and perioperative conditions were matched using nonparsimonious multivariate logistic regression. The perioperative conditions included age, gender, BMI, ASA physical status, operation type, diversion type, tumor size, and neoadjuvant chemotherapy. Pathological stage and grade, surgical margin positivity, LVI, carcinoma in situ (CIS), number of removed lymph nodes, number of positive lymph nodes, adjuvant chemotherapy, and radiotherapy were excluded from propensity matching because these variables cannot be used to determine the preoperative condition. A total of 305 patients with high AST/ALT ratios were matched in a 1:1 ratio to 466 patients with low AST/ALT ratios using the nearest neighbor method with 0.02 calibration. The propensity score matching was well calibrated and differentiated in most items with a standardized mean difference of less than 0.05.

All statistical tests were performed using IBM SPSS Statistics, version 22.0 (IBM, Armonk, NY, USA), and a  $P$  value of  $<0.05$  was considered to indicate statistical significance.

## 3. Results

**3.1. Clinical and Pathological Characteristics of Patients.** A total of 771 patients diagnosed with UC in the bladder who underwent radical cystectomy were included. The median follow-up was 84 months (IQR 36–275). Of the total patients, 84.5% were men and the mean age was 64.8 years

TABLE 1: Clinicopathological characteristics of patients before and after propensity score matching.

Variables	Before propensity score matching		<i>P</i> value	After propensity score matching		<i>P</i> value
	Low AST/ALT ( <i>N</i> = 466)	High AST/ALT ( <i>N</i> = 305)		Low AST/ALT ( <i>N</i> = 305)	High AST/ALT ( <i>N</i> = 305)	
Mean age (year)	62.9 ± 9.9	67.2 ± 10.0	<0.001	64.6 ± 8.8	67.2 ± 10.0	0.001
Gender			<0.001			<0.001
Female	45 (9.6%)	74 (24.3%)		31 (10.2%)	74 (24.3%)	
Male	421 (90.4%)	231 (75.7%)		274 (89.8%)	231 (75.7%)	
BMI (kg/m <sup>2</sup> )	23.7 ± 3.8	22.2 ± 2.9	<0.001	23.0 ± 2.7	22.2 ± 2.9	0.067
ASA			0.373			0.714
1	172 (36.9%)	103 (33.7%)		110 (36.0%)	103 (33.7%)	
2	275 (59.0%)	182 (59.7%)		180 (59.0%)	182 (59.7%)	
≥3	19 (4.1%)	20 (6.6%)		15 (4.9%)	20 (6.6%)	
Operative type			0.218			0.273
Open	424 (91.0%)	285 (93.5%)		295 (93.4%)	285 (93.5%)	
Laparoscopic	24 (5.2%)	16 (5.2%)		11 (3.6%)	16 (5.2%)	
Robot	18 (3.8%)	4 (1.3%)		9 (3.0%)	4 (1.3%)	
Diversion type			0.052			0.168
Conduit	253 (54.3%)	194 (63.6%)		209 (68.5%)	194 (63.6%)	
Neobladder	213 (45.7%)	111 (36.4%)		96 (31.5%)	111 (36.4%)	
Tumor grade			0.396			0.569
Low	12 (2.6%)	11 (3.6%)		10 (3.3%)	11 (3.6%)	
High	454 (97.4%)	294 (96.4%)		295 (96.7%)	294 (96.4%)	
Tumor size (cm)	2.4 ± 3.0	3.3 ± 3.2	0.017	1.2 ± 2.4	3.3 ± 3.2	0.058
Pathological T stage			0.002			0.112
T1	73 (15.7%)	57 (18.7%)		53 (17.4%)	57 (18.7%)	
T2	264 (56.7%)	122 (40.0%)		156 (51.0%)	122 (40.1%)	
T3	106 (22.7%)	104 (34.1%)		80 (26.2%)	104 (34.1%)	
T4	23 (4.9%)	22 (7.2%)		16 (5.2%)	22 (7.2%)	
Margin positive	7 (1.5%)	15 (4.9%)	0.036	5 (1.6%)	15 (4.9%)	0.041
LVI	129 (27.6%)	106 (34.8%)	0.055	90 (29.5%)	106 (34.8%)	0.193
CIS	155 (33.3%)	97 (31.8%)	0.735	97 (31.8%)	97 (31.8%)	1.000
Pathological N stage			0.455			0.544
N0	382 (82.0%)	240 (78.7%)		252 (82.6%)	240 (78.7%)	
N1	34 (7.3%)	20 (6.6%)		20 (6.6%)	20 (6.6%)	
N2	42 (9.0%)	38 (12.5%)		28 (9.2%)	38 (12.5%)	
N3	8 (1.7%)	7 (2.3%)		5 (1.6%)	7 (2.3%)	
Removed LN	18.9 ± 11.7	16.9 ± 10.9	0.018	17.1 ± 11.5	16.9 ± 10.9	0.158
Positive LN	0.7 ± 2.5	1.0 ± 3.0	0.199	0.6 ± 2.3	1.0 ± 3.0	0.146
Pathological M stage			0.749			0.966
M0	462 (99.2%)	304 (99.7%)		363 (99.2%)	304 (99.7%)	
M1	4 (0.8%)	1 (0.3%)		2 (0.7%)	1 (0.3%)	
NACH	64 (13.7%)	39 (12.8%)	0.827	40 (13.1%)	39 (12.8%)	0.976
ACH	99 (21.2%)	74 (24.3%)	0.414	65 (21.3%)	74 (24.3%)	0.440
ART	4 (0.8%)	3 (1.0%)	0.986	3 (1.0%)	3 (1.0%)	1.000
Recurrence rate	139 (29.8%)	115 (37.7%)	0.037	89 (29.2%)	115 (37.7%)	0.032
Mortality	141 (30.3%)	140 (45.9%)	<0.001	96 (31.5%)	140 (45.9%)	<0.001
Cancer-caused mortality	88 (18.9%)	96 (31.5%)	<0.001	59 (19.3%)	96 (31.5%)	0.001
AST/ALT ratio	0.9 ± 0.2	1.7 ± 1.6	<0.001	0.9 ± 0.2	1.7 ± 1.6	<0.001

ASA: American Society of Anesthesiologists; BMI: body mass index; NACH: neoadjuvant chemotherapy; ALT: alanine aminotransferase; AST: aspartate aminotransferase; LVI: lymphovascular invasion; CIS: carcinoma in situ; LN: lymph node; NACH: neoadjuvant chemotherapy; ACH: adjuvant chemotherapy; ART: adjuvant radiotherapy.

(SD  $\pm$  10.2). Most patients (91.9%) received open radical cystectomy. Table 1 shows the clinical and pathological characteristics of the patients. Patients were divided into two groups based on an AST/ALT ratio of 1:1. The mean age of the high AST/ALT group was significantly higher than that of the low AST/ALT group ( $P < 0.001$ ). In addition, the tumor size was larger ( $P = 0.017$ ) in the high AST/ALT group. In the pathological T stage, T2 was relatively low in the AST/ALT group, while T3 and T4 were high in the AST/ALT group. In the pathological T stage, T2 was relatively higher in the low AST/ALT group. However, T3 and T4 were higher in the high AST/ALT group ( $P = 0.002$ ). The surgical margin positive rate was higher in the high AST/ALT group ( $P = 0.036$ ), and the number of removed lymph nodes was higher in the low AST/ALT group ( $P = 0.018$ ). The recurrence rate in the high AST/ALT group was higher than that in the low AST/ALT group ( $P = 0.037$ ). Overall, bladder cancer-caused mortality was also higher in the high AST/ALT group than in the low AST/ALT group ( $P < 0.001$ ). After the propensity score matching, 1:1 matching was performed for age, gender, BMI, ASA physical status, operation type, diversion type, tumor size, removed lymph node, and neoadjuvant chemotherapy. The propensity score matching was 1:1 matched for age, gender, BMI, ASA physical status, operation type, diversion type, tumor size, and neoadjuvant chemotherapy. The propensity score matching was well calibrated and differentiated in most items. However, the mean age and gender were not well matched because of the limited number of populations.

**3.2. Correlation between Serum Preoperative AST/ALT Ratio and Oncologic and Survival Outcomes before Propensity Score Matching.** The overall mortality rate was significantly higher (45.9%) in the high AST/ALT group ( $P < 0.001$ ) than in the low AST/ALT group (30.3%). The cancer-causing mortality rate and recurrence rate were also significantly higher in the high AST/ALT group ( $P < 0.001$  and  $P = 0.037$ , respectively) (Table 1). Kaplan–Meier analysis shows that the low AST/ALT group has a better prognosis for OS ( $P < 0.001$ ), CSS ( $P < 0.001$ ), and RFS ( $P = 0.001$ ) than the high AST/ALT group (Figures 1(a)–1(c)). The multivariate Cox analysis showed that a high preoperative AST/ALT ratio was a significant independent predictor of poor prognosis such as OS (HR 2.05, 95% CI 1.65–2.56,  $P = 0.007$ ) and CSS (HR 1.32, 95% CI 0.69–2.56,  $P < 0.001$ ) (Table 2). In addition, the tumor size, high tumor grade, and pathological T and N stages are associated with poor prognosis (Table 2).

**3.3. After Propensity Score Matching.** The overall mortality rate was significantly higher (45.9%) in the high AST/ALT group ( $P < 0.001$ ) than in the low AST/ALT group (31.5%). The cancer-causing mortality rate and recurrence rate were also significantly higher in the high AST/ALT group ( $P = 0.001$  and  $P < 0.001$ , respectively) (Table 1). Kaplan–Meier analysis shows that the low AST/ALT group has a better prognosis for OS ( $P < 0.001$ ), CSS ( $P < 0.001$ ), and RFS ( $P = 0.001$ ) than the high AST/ALT group (Figures 1(d)–1(f)). The multivariate Cox analysis showed that a high preoperative AST/ALT ratio was a significant

independent predictor of poor prognosis such as OS (HR 1.57, 95% CI 1.20–2.06,  $P = 0.001$ ), CSS (HR 1.76, 95% CI 1.26–2.48,  $P = 0.001$ ), and RFS (HR 1.53, 95% CI 1.15–2.05,  $P = 0.004$ ) (Table 3). In addition, the tumor size, high tumor grade, and pathological T, N, and M stages are also associated with poor prognosis. The NACH was associated with good prognosis (Table 3).

## 4. Discussion

In our present study, patients with high AST/ALT ratio showed significant association with poor prognosis in clinical outcomes. We analyzed patients who underwent radical cystectomy for MIBC or high-risk bladder cancer intolerant to intravesical BCG treatment. The number of patients was 617 in 24 years. The cohort was relatively large, and the follow-up period was relatively long. We performed a 1:1 propensity matching of preoperative factors, except for the AST/ALT ratio to compensate for the bias due to preoperative factors. Due to the limited number of patients, one-to-many propensity matching could not be performed. Propensity matching was not satisfactory, but preoperative factors except mean age and gender matched. Increased AST/ALT ratio before radical cystectomy is a negatively prognostic factor. Preoperative high AST/ALT group has a poor prognosis for OS ( $P < 0.001$ ), CSS ( $P < 0.001$ ), and RFS ( $P = 0.004$ ) than the low AST/ALT group. And preoperative AST/ALT ratio is a significant prognostic factor of postoperative oncologic outcomes. The matched results also show that a preoperative high AST/ALT ratio is negatively correlated with survival outcomes such as OS (HR 1.57, 95% CI 1.20–2.06,  $P = 0.001$ ), CSS (HR 1.76, 95% CI 1.26–2.48,  $P = 0.001$ ), and RFS (HR 1.53, 95% CI 1.15–2.05,  $P = 0.004$ ).

AST/ALT ratio has been reported as a predictor of prognosis in lung cancer, colorectal cancer, pancreatic cancer, breast cancer, and kidney cancer [12–16]. Rawson and Peto conducted a retrospective analysis of 3873 patients with small cell lung cancer. The AST and AST/ALT ratios were considered to be important prognostic indexes [15]. Stoken et al. analyzed the prognostic factors of pancreatic cancer in 653 patients and reported the effect of AST as a prognostic factor [16]. Bezan et al. analyzed 698 patients retrospectively. They reported that the AST/ALT ratio is an independent prognostic factor related to poor prognosis of metastasis-free survival (HR 1.61, 95% CI 1.25–2.07,  $P < 0.001$ ) and OS (HR 1.76, 95% CI 1.34–2.32,  $P < 0.001$ ) in patients with nonmetastatic renal cell carcinoma [18]. Lee et al. analyzed retrospectively 2965 patients with nonmetastatic renal cell carcinoma (RCC). The AST/ALT ratio of 1:2 or more was the predictor of poor prognosis of disease progression (HR 1.37, 95% CI 1.00–1.88,  $P = 0.048$ ), overall mortality (HR 1.56, 95% CI 1.07–2.27,  $P = 0.021$ ), and cancer-specific mortality (HR 1.97, 95% CI 1.25–3.12,  $P = 0.004$ ) [22]. In Chougule's study, 92 neck cancer patients without liver metastases and 71 uterine cervix cancer patients had increased AST and ALT values from 133% to 229% of normal value, which decreased to a normal level after radiotherapy [23]. In the O'Reilly et al. study of 312 breast cancer patients, 84% of the patients had biochemical abnormalities in AST, and the elevation levels

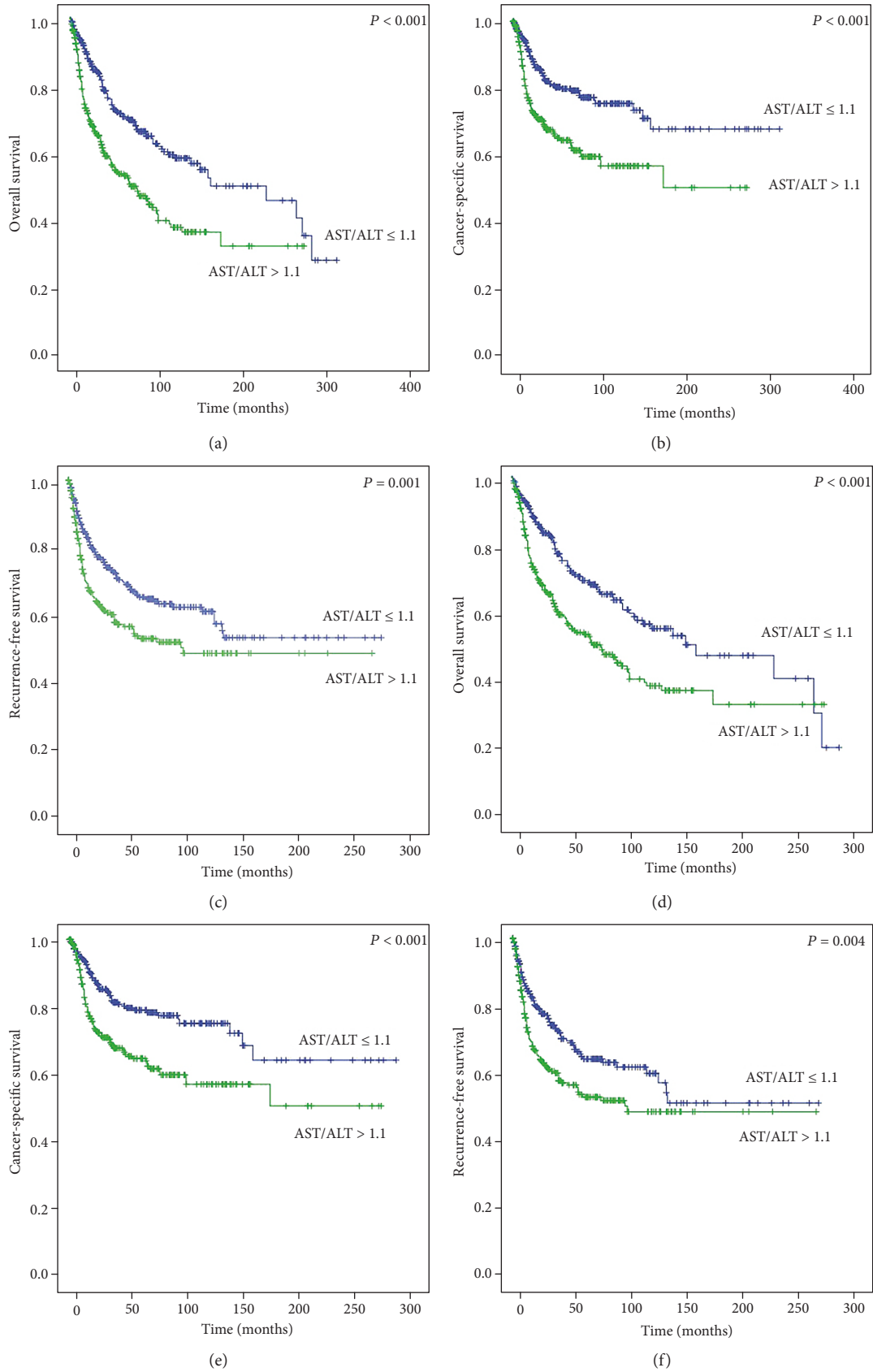


FIGURE 1: Kaplan–Meier survival curves of overall survival, cancer-specific survival, and recurrence-free survival according to the preoperative aspartate transaminase (AST)/alanine transaminase (ALT) ratio before (a–c) and after (d–f) propensity score matching.

TABLE 2: Multivariate Cox proportional hazards analyses of AST/ALT ratio on overall survival, cancer-specific survival, and recurrence-free survival.

Variables	Overall survival		Cancer-specific survival		Recurrence-free survival	
	HR (95% CI)	<i>P</i> value	HR (95% CI)	<i>P</i> value	HR (95% CI)	<i>P</i> value
Age	1.03 (1.00-1.01)	0.032	1.05 (1.01-1.09)	0.022	1.01 (0.97-1.04)	0.633
BMI	0.92 (0.84-1.01)	0.099	0.92 (0.84-1.02)	0.103	1.06 (1.00-1.13)	0.043
Tumor size	1.16 (1.09-1.24)	<0.001	1.16 (1.09-1.24)	<0.001	1.13 (1.07-1.20)	<0.001
High tumor grade	1.58 (1.10-2.28)	0.013	1.65 (1.09-2.49)	0.017	1.30 (0.90-1.88)	0.159
≥pT2 stage	3.30 (1.18-9.21)	0.022	5.78 (2.51-13.35)	<0.001	5.14 (2.05-12.90)	<0.001
≥N1 stage	1.37 (1.06-1.77)	0.014	1.35 (1.05-1.74)	0.018	1.54 (1.20-1.97)	<0.001
≥M1 stage	1.68 (0.23-11.99)	0.605	3.89 (0.45-33.90)	0.219	1.73 (0.22-13.58)	0.604
NACH	1.21 (0.60-2.42)	0.594	1.33 (0.63-2.78)	0.191	1.86 (0.80-4.26)	0.142
AST/ALT ratio						
AST/ALT ≤1.1	Reference		Reference		Reference	
AST/ALT >1.1	2.15 (1.23-3.73)	0.007	2.05 (1.65-2.56)	<0.001	1.32 (0.69-2.56)	0.087

BMI: body mass index; NACH: neoadjuvant chemotherapy; ALT: alanine aminotransferase; AST: aspartate aminotransferase.

TABLE 3: Multivariate Cox proportional hazards analyses of AST/ALT ratio on overall survival, cancer-specific survival, and recurrence-free survival after propensity score matching.

Variables	Overall survival		Cancer-specific survival		Recurrence-free survival	
	HR (95% CI)	<i>P</i> value	HR (95% CI)	<i>P</i> value	HR (95% CI)	<i>P</i> value
Age	1.03 (1.01-1.04)	<0.001	1.02 (0.99-1.03)	0.092	1.00 (0.99-1.02)	0.876
BMI	0.92 (0.87-0.96)	<0.001	0.94 (0.88-0.99)	0.034	0.97 (0.92-1.02)	0.299
Tumor size	1.09 (1.05-1.15)	<0.001	1.11 (1.05-1.17)	<0.001	1.09 (1.04-1.14)	0.001
High tumor grade	1.51 (1.04-2.18)	0.018	1.70 (1.13-2.55)	0.010	1.37 (0.95-1.98)	0.093
≥pT2 stage	5.36 (2.12-13.51)	<0.001	6.99 (3.00-16.28)	<0.001	13.47 (4.25-42.65)	<0.001
≥N1 stage	1.36 (1.05-1.75)	0.018	1.35 (1.05-1.74)	0.018	1.60 (1.25-2.06)	0.002
≥M1 stage	1.27 (0.74-2.18)	0.394	1.71 (0.98-3.00)	0.060	2.10 (1.23-3.60)	0.007
NACH	0.51 (0.35-0.75)	0.001	0.45 (0.29-0.69)	<0.001	0.47 (0.32-0.67)	<0.001
AST/ALT ratio						
AST/ALT ≤1.1	Reference	Reference	Reference	Reference	Reference	Reference
AST/ALT >1.1	1.57 (1.20-2.06)	0.001	1.76 (1.26-2.48)	0.001	1.53 (1.15-2.05)	0.004

BMI: body mass index; NACH: neoadjuvant chemotherapy; ALT: alanine aminotransferase; AST: aspartate aminotransferase.

of AST were associated with an important association of survival ( $P < 0.001$ ) [24]. In the case of UC, Lee et al. retrospectively analyzed 623 UTUC patients who underwent nephroureterectomy [20]. Elevated preoperative AST/ALT is a poor prognostic factor for the postoperative survival outcome of UTUC. The postoperative survival outcomes were PFS (HR 2.33, 95% CI 1.63-3.34,  $P < 0.001$ ), CSS (HR 2.55, CI 1.69-3.85;  $P < 0.001$ ), and OS (HR 2.07, 95% CI 1.41-3.03,  $P < 0.001$ ). Gorgel et al. retrospectively analyzed 153 patients who underwent radical cystectomy [25]. The preoperative AST/ALT ratio was a significant prognostic factor for OS (HR 2.61, 95% CI 1.49-4.56,  $P < 0.001$ ) and disease-free survival (HR 5.79, 95% CI 2.25-15.13,  $P < 0.001$ ). Pathological T stage and age were correlated with prognosis. In addition, the AST/ALT ratio cutoff value was 1.3. In our study, the size of the tumor, neoadjuvant chemotherapy, and type of diversion were correlated with prognosis. The AST/ALT ratio cutoff value was 1.1. Ha et al. retrospectively analyzed

118 patients who underwent radical cystectomy. A high AST/ALT ratio was a poor prognostic factor for metastasis-free survival (HR 2.39, 95% CI 1.16-4.91,  $P = 0.018$ ), CSS (HR 2.75, 95% CI 1.21-6.25,  $P = 0.015$ ), and OS (HR 2.76, 95% CI 1.26-6.07,  $P = 0.011$ ). The AST/ALT ratio cutoff value was 1.3 [26].

Several hypotheses have been presented to explain the association of the AST/ALT ratio with cancer. The most well-known of these hypotheses is the “Warburg effect.” In cancer cell metabolism, glucose uptake and anaerobic glycolysis are increased for the ATP production of adenosine triphosphatase (ATP) [27]. Cancer cells produce sufficient ATP through glycolysis metabolism, thereby promoting the multiplying of cancer cells. In addition, increased glycolysis reduces pH and increases lactate secretion. Reduced pH affects the tumor microenvironment and has a favorable effect on cancer progression, metastasis, and local invasion [28, 29]. Also, increased lactate has been suggested to play



an important role in maintaining glycolysis, affecting the lactate dehydrogenase and nicotinamide adenine dinucleotide (NADH)/NAD<sup>+</sup> ratio, and affecting the glucose transporter [30]. The AST plays an important role in glycolysis by relocating NADH to mitochondria.

UC is known to be associated with glucose metabolism [31, 32]. In addition, Whyard et al. reported fluorescence microscopy to show the difference in glucose consumption between urothelium and malignant urothelial cells [32]. Therefore, although AST and ALT are associated with UC, the mechanism of the association between the UC and AST/ALT ratios is still unclear and further research is needed.

The present study has several limitations. Retrospective research design can have an inherent bias. In addition, the undetectable illness, the condition of the patient, and medications currently taken by the patient may have affected AST and ALT. Finally, our target population was confined to Korean patients and could therefore not reflect the differences among patients according to race. Further research and prospective studies are needed to verify our results.

## 5. Conclusions

Increased AST/ALT ratio before radical cystectomy is a negatively prognostic factor that has a significant effect on the postoperative survival of bladder UC patients. Additional prospective studies are needed to identify the specific mechanisms for bladder UC and AST/ALT ratio.

## Data Availability

The data used to support the findings of this study are available from the corresponding author upon request.

## Disclosure

No funders had any role in the study concept and design, experiments, analysis of data, or decision for publication or in writing the manuscript.

## Conflicts of Interest

The authors declare that they have no conflicts of interest.

## Acknowledgments

This study was supported by the National Research Foundation of Korea (NRF) grant funded by the Korea government (MOE) (Grant number: 2016R1A2B4011623).

## References

- [1] L. A. Torre, F. Bray, R. L. Siegel, J. Ferlay, J. Lortet-Tieulent, and A. Jemal, "Global cancer statistics, 2012," *CA: a Cancer Journal for Clinicians*, vol. 65, no. 2, pp. 87–108, 2015.
- [2] J. Ferlay, I. Soerjomataram, R. Dikshit et al., "Cancer incidence and mortality worldwide: sources, methods and major patterns in GLOBOCAN 2012," *International Journal of Cancer*, vol. 136, no. 5, pp. E359–E386, 2015.
- [3] M. Babjuk, A. Böhle, M. Burger et al., "EAU guidelines on non-muscle-invasive urothelial carcinoma of the bladder: update 2016," *European Urology*, vol. 71, no. 3, pp. 447–461, 2017.
- [4] A. M. Kamat, J. A. Witjes, M. Brausi et al., "Defining and treating the spectrum of intermediate risk nonmuscle invasive bladder cancer," *The Journal of Urology*, vol. 192, no. 2, pp. 305–315, 2014.
- [5] R. J. Sylvester, A. P. M. van der Meijden, W. Oosterlinck et al., "Predicting recurrence and progression in individual patients with stage Ta T1 bladder cancer using EORTC risk tables: a combined analysis of 2596 patients from seven EORTC trials," *European Urology*, vol. 49, no. 3, pp. 466–477, 2006.
- [6] G. Poli, G. Cochetti, A. Boni, M. G. Egidi, S. Brancorsini, and E. Mearini, "Characterization of inflammasome-related genes in urine sediments of patients receiving intravesical BCG therapy," *Urologic Oncology*, vol. 35, no. 12, pp. 674.e19–674.e24, 2017.
- [7] J. P. Stein, G. Lieskovsky, R. Cote et al., "Radical cystectomy in the treatment of invasive bladder cancer: long-term results in 1,054 patients," *Journal of Clinical Oncology*, vol. 19, no. 3, pp. 666–675, 2001.
- [8] G. Poli, S. Brancorsini, G. Cochetti, F. Barillaro, M. G. Egidi, and E. Mearini, "Expression of inflammasome-related genes in bladder cancer and their association with cytokeratin 20 messenger RNA," *Urologic Oncology*, vol. 33, no. 12, pp. 505.e1–505.e7, 2015.
- [9] F. Soria, M. J. Droller, Y. Lotan et al., "An up-to-date catalog of available urinary biomarkers for the surveillance of non-muscle invasive bladder cancer," *World Journal of Urology*, vol. 36, no. 12, pp. 1981–1995, 2018.
- [10] A. Carobene, F. Braga, T. Roraas, S. Sandberg, and W. A. Bartlett, "A systematic review of data on biological variation for alanine aminotransferase, aspartate aminotransferase and  $\gamma$ -glutamyl transferase," *Clinical Chemistry and Laboratory Medicine*, vol. 51, no. 10, pp. 1997–2007, 2013.
- [11] A. Karmen, F. Wroblewski, and J. S. Ladue, "Transaminase activity in human blood," *The Journal of Clinical Investigation*, vol. 34, no. 1, pp. 126–133, 1955.
- [12] M. Botros and K. A. Sikaris, "The De Ritis ratio: the test of time," *Clinical Biochemist Reviews*, vol. 34, no. 3, pp. 117–130, 2013.
- [13] T. Kiba, T. Ito, T. Nakashima et al., "Bortezomib and dexamethasone for multiple myeloma: higher AST and LDH levels associated with a worse prognosis on overall survival," *BMC Cancer*, vol. 14, no. 1, p. 462, 2014.
- [14] G. Lindmark, B. Gerdin, L. Pählman, R. Bergström, and B. Glimelius, "Prognostic predictors in colorectal cancer," *Diseases of the Colon and Rectum*, vol. 37, no. 12, pp. 1219–1227, 1994.
- [15] A report from the Subcommittee for the Management of Lung Cancer of the United Kingdom Coordinating Committee on Cancer Research, N. S. B. Rawson, and J. Peto, "An overview of prognostic factors in small cell lung cancer," *British Journal of Cancer*, vol. 61, no. 4, pp. 597–604, 1990.
- [16] D. D. Stocken, A. B. Hassan, D. G. Altman et al., "Modelling prognostic factors in advanced pancreatic cancer," *British Journal of Cancer*, vol. 99, no. 6, pp. 883–893, 2008.
- [17] F. De Ritis, M. Coltorti, and G. Giusti, "An enzymic test for the diagnosis of viral hepatitis; the transaminase serum

- activities," *Clinica Chimica Acta*, vol. 2, no. 1, pp. 70–74, 1957.
- [18] A. Bezan, E. Mrcic, D. Krieger et al., "The preoperative AST/ALT (De Ritis) ratio represents a poor prognostic factor in a cohort of patients with nonmetastatic renal cell carcinoma," *The Journal of Urology*, vol. 194, no. 1, pp. 30–35, 2015.
- [19] Y. S. Tai, C. H. Chen, C. Y. Huang, H. C. Tai, S. M. Wang, and Y. S. Pu, "Diabetes mellitus with poor glycemic control increases bladder cancer recurrence risk in patients with upper urinary tract urothelial carcinoma," *Diabetes/Metabolism Research and Reviews*, vol. 31, no. 3, pp. 307–314, 2015.
- [20] H. Lee, Y. H. Choi, H. H. Sung et al., "De Ritis ratio (AST/ALT) as a significant prognostic factor in patients with upper tract urothelial cancer treated with surgery," *Clinical Genitourinary Cancer*, vol. 15, no. 3, pp. e379–e385, 2017.
- [21] C. W. Jeong, J. Suh, H. D. Yuk et al., "Establishment of the Seoul National University prospectively enrolled registry for genitourinary cancer (SUPER-GUC): a prospective, multidisciplinary, bio-bank linked cohort and research platform," *Investigative and Clinical Urology*, vol. 60, no. 4, pp. 235–243, 2019.
- [22] H. Lee, S. E. Lee, S. S. Byun, H. H. Kim, C. Kwak, and S. K. Hong, "De Ritis ratio (aspartate transaminase/alanine transaminase ratio) as a significant prognostic factor after surgical treatment in patients with clear-cell localized renal cell carcinoma: a propensity score-matched study," *BJU International*, vol. 119, no. 2, pp. 261–267, 2017.
- [23] A. Chougule, S. Hussain, and D. P. Agarwal, "Prognostic and diagnostic value of serum pseudocholinesterase, serum aspartate transaminase, and serum alinine transaminase in malignancies treated by radiotherapy," *Journal of Cancer Research and Therapeutics*, vol. 4, no. 1, pp. 21–25, 2008.
- [24] S. M. O'Reilly, M. A. Richards, and R. D. Rubens, "Liver metastases from breast cancer: the relationship between clinical, biochemical and pathological features and survival," *European Journal of Cancer*, vol. 26, no. 5, pp. 574–577, 1990.
- [25] S. N. Gorgel, O. Kose, E. M. Koc, E. Ates, Y. Akin, and Y. Yilmaz, "The prognostic significance of preoperatively assessed AST/ALT (De Ritis) ratio on survival in patients underwent radical cystectomy," *International Urology and Nephrology*, vol. 49, no. 9, pp. 1577–1583, 2017.
- [26] Y. S. Ha, S. W. Kim, S. Y. Chun et al., "Association between De Ritis ratio (aspartate aminotransferase/alanine aminotransferase) and oncological outcomes in bladder cancer patients after radical cystectomy," *BMC Urology*, vol. 19, no. 1, p. 10, 2019.
- [27] O. Warburg, "On respiratory impairment in cancer cells," *Science*, vol. 124, no. 3215, pp. 269–270, 1956.
- [28] D. M. Brizel, T. Schroeder, R. L. Scher et al., "Elevated tumor lactate concentrations predict for an increased risk of metastases in head-and-neck cancer," *International Journal of Radiation Oncology, Biology, Physics*, vol. 51, no. 2, pp. 349–353, 2001.
- [29] S. Walenta, T. V. Chau, T. Schroeder et al., "Metabolic classification of human rectal adenocarcinomas: a novel guideline for clinical oncologists?," *Journal of Cancer Research and Clinical Oncology*, vol. 129, no. 6, pp. 321–326, 2003.
- [30] A. Dorward, S. Sweet, R. Moorehead, and G. Singh, "Mitochondrial contributions to cancer cell physiology: redox balance, cell cycle, and drug resistance," *Journal of Bioenergetics and Biomembranes*, vol. 29, no. 4, pp. 385–392, 1997.
- [31] K. Kitajima, S. Yamamoto, K. Fukushima et al., "FDG-PET/CT as a post-treatment restaging tool in urothelial carcinoma: comparison with contrast-enhanced CT," *European Journal of Radiology*, vol. 85, no. 3, pp. 593–598, 2016.
- [32] T. Whyard, W. C. Waltzer, D. Waltzer, and V. Romanov, "Metabolic alterations in bladder cancer: applications for cancer imaging," *Experimental Cell Research*, vol. 341, no. 1, pp. 77–83, 2016.

## Research Article

# CSF-1 Overexpression Predicts Poor Prognosis in Upper Tract Urothelial Carcinomas

Wei-Chi Hsu <sup>1,2</sup>, Yi-Chen Lee <sup>1,3</sup>, Peir-In Liang,<sup>4</sup> Lin-Li Chang <sup>1,5</sup>, A-Mei Huang <sup>1,6,7</sup>, Hui-Hui Lin <sup>2</sup>, Wen-Jeng Wu <sup>1,2,8</sup>, Ching-Chia Li <sup>2</sup>, Wei-Ming Li,<sup>2,8,9</sup> Jhen-Hao Jhan <sup>2</sup>, and Hung-Lung Ke <sup>1,2,8</sup>

<sup>1</sup>Graduate Institute of Medicine, College of Medicine, Kaohsiung Medical University, Kaohsiung, Taiwan

<sup>2</sup>Department of Urology, Kaohsiung Medical University Hospital, Kaohsiung Medical University, Kaohsiung, Taiwan

<sup>3</sup>Department of Anatomy, School of Medicine, College of Medicine, Kaohsiung Medical University, Kaohsiung, Taiwan

<sup>4</sup>Department of Pathology, Kaohsiung Medical University Hospital, Kaohsiung Medical University, Kaohsiung, Taiwan

<sup>5</sup>Department of Microbiology and Immunology, School of Medicine, College of Medicine, Kaohsiung Medical University, Kaohsiung, Taiwan

<sup>6</sup>Department of Biochemistry, School of Medicine, College of Medicine, Kaohsiung Medical University, Kaohsiung, Taiwan

<sup>7</sup>Graduate Institute of Clinical Medicine, College of Medicine, Kaohsiung Medical University, Kaohsiung, Taiwan

<sup>8</sup>Department of Urology, School of Medicine, College of Medicine, Kaohsiung Medical University, Kaohsiung, Taiwan

<sup>9</sup>Department of Urology, Ministry of Health and Welfare Pingtung Hospital, Pingtung, Taiwan

Correspondence should be addressed to Hung-Lung Ke; [hunglungke@gmail.com](mailto:hunglungke@gmail.com)

Received 18 April 2019; Accepted 25 June 2019; Published 21 August 2019

Guest Editor: Giovanni Cochetti

Copyright © 2019 Wei-Chi Hsu et al. This is an open access article distributed under the Creative Commons Attribution License, which permits unrestricted use, distribution, and reproduction in any medium, provided the original work is properly cited.

**Background.** Colony-stimulating factor-1 (CSF-1) is a homodimeric glycoprotein. The main role of CSF-1 is as a hematopoietic growth factor that modulates proliferation, differentiation, and survival of macrophages. Moreover, CSF-1 has also been reported to be aberrantly expressed in several human cancers. However, the precise role of CSF-1 in upper tract urothelial carcinomas (UTUC) has not been studied. In this research, we examined the clinical significance of CSF-1 expression in UTUC. **Materials and Methods.** One hundred twelve cancer tissue samples of UTUC from patients were included in this study, and the other cohort of 35 UTUC were paired cancer-adjacent normal samples. CSF-1 expression was evaluated by immunohistochemistry, and the association of CSF-1 expression with different clinicopathological variables was analyzed. **Results.** CSF-1 expression was higher in UTUC than in the normal urothelium ( $P=0.005$ ). The CSF-1 expression was primarily localized in the nucleus and was significantly correlated with tumor size ( $P=0.04$ ) and patients who had a high stage ( $P<0.001$ ), distant metastasis ( $P=0.006$ ), recurrence ( $P=0.003$ ), and cancer death ( $P=0.005$ ). High CSF-1 expression was correlated with poor disease-free survival ( $P=0.008$ ) and cancer-specific survival ( $P=0.001$ ). Our results also used univariate and multivariable analyses, which found that high CSF-1 expression was an independent predictor of poor disease-free survival (hazard ratio = 2.56;  $P=0.007$ ) and cancer-specific survival (hazard ratio = 5.14;  $P=0.022$ ). **Conclusions.** Our findings indicate that the expression of CSF-1 is a potential prognostic marker for predicting patient survival and recurrence in UTUC.

## 1. Introduction

Urothelial carcinomas (UC) can be categorized into three groups: bladder (UCB), renal pelvis, and ureter [1]. Upper tract urothelial carcinomas (UTUC) includes both ureteral and renal pelvic tumors [2]. UTUC is a rare cancer with vastly different characteristics between eastern and western

countries; e.g., the male-to-female ratio is 1 : 1.2 in Taiwanese UTUC patients [3] but the ratio of patients in western countries is reversed [4]. In western countries, the incidence of urothelial carcinomas presenting as UCB is 90-95% [5], while UTUC is rare, accounting for only 5-10% of all urothelial carcinomas [6-8]. However, the incidence of UTUC in Taiwan is markedly higher at 30% of all urothelial carcinomas [9].



It is probable that various genetic, environmental, and other risk factors lead to a higher incidence of UTUC in Taiwan [10, 11]. The main predicting factor for prognosis is the cancer stage [12]. However, even in the same pathological stage and with standard treatment, patients still have divergent prognoses. Our previous studies have demonstrated some possible prognostic biomarkers such as hypoxia-induced factor 1 $\alpha$  (HIF-1 $\alpha$ ) [13], leptin receptor [14], and signal transducer and activator of transcription 3 (STAT3) [15] associated with UTUC. However, the exact molecular mechanism of UTUC progression is not widely understood, and therefore, no probable prognostic markers have been proven.

Colony-stimulating factor-1 (CSF-1), also called “macrophage colony-stimulating factor” (M-CSF), is an important hematopoietic growth factor. CSF-1 binds to its receptor—the colony-stimulating factor-1 receptor (CSF-1R/c-fms)—and regulates the survival, differentiation, and proliferation of the monocyte-macrophage lineage [16, 17]. Additionally, several studies reveal that CSF-1 can promote tumor cell progression, migration, invasion, and metastasis [18–21]. CSF-1 is produced by macrophages, fibroblasts, and epithelial cells and is also secreted by tumor cells. Overexpression of CSF-1 has been associated with several human cancers, including breast cancers [22, 23], renal cell carcinomas [24], and ovarian cancers [25]. Moreover, clinical studies have shown that high CSF-1 levels have been linked to a poor prognosis in pancreatic cancer [26], prostate cancer [27], colorectal cancer [28], and clear-cell renal cell carcinoma [29].

Because there is no published research investigating the role of CSF-1 in UTUC, we aim to examine the association between the clinicopathological behavior of UTUC and CSF-1 expression in cancer tissues.

## 2. Materials and Methods

**2.1. Surgical Specimens and Clinicopathological Data.** One hundred twelve formalin-fixed UTUC tissues and thirty-five paired noncancerous urothelial samples were obtained from the Department of Urology, Kaohsiung Medical University Hospital, from 1997 to 2006 as previously described [14, 15]. All samples were histologically confirmed to be UC. All patients were treated with nephroureterectomy and excision of the bladder cuff. Medical records were reviewed retrospectively and clinicopathological data were retrieved. A follow-up protocol was created according to the National Comprehensive Cancer Network (NCCN) guidelines. The median follow-up time was 40.39 months, and the range was between 1 and 136 months. Disease-free survival was calculated from the date of surgery to the date of UTUC recurrence. Cancer-specific survival was defined as the time from the date of surgery to the date of cancer death. The pathologic grade was classified according to the World Health Organization (WHO) histologic criteria, and tumor staging was determined according to the Union for International Cancer Control tumor-node-metastasis classification. The clinicopathological parameters were obtained by retrospectively reviewing medical records. An informed consent was provided to the patient and signed before surgery. The

study protocol was reviewed and approved by the Institutional Review Board of Kaohsiung Medical University Hospital (KMUH-IRB-E(II)-20170070).

**2.2. Immunohistochemical Staining of CSF-1.** Four-micrometer-thick sections from paraffin-embedded blocks were cut onto precoated slides, followed by deparaffinization, rehydration, and antigen retrieval as previously described [14, 15]. Endogenous peroxidase was blocked per the manufacturer’s protocol (Dako, Carpinteria, CA). The slides were incubated with an anti-CSF-1 monoclonal antibody (MABF191, Merck Millipore) at a 1 : 200 dilution at 4°C for 1 h. Primary antibodies were detected using the Dako ChemMate EnVision Kit (K5001, Dako, Carpinteria, CA). Finally, the slides were counterstained with hematoxylin and investigated by light microscopy.

**2.3. Evaluation of Immunohistochemical Staining.** Scoring for CSF-1-positive staining was decided based on the percentage of positively stained cells in 4 quantitative categories as previously described [14, 15]: score 1, <25% positive cells; score 2, 26% to 50% positive cells; score 3, 51% to 75% positive cells; and score 4, >76% positive cells. The cancer immunostaining was inspected by 2 qualified pathologists who were blinded to the clinical status of the patients. Any discrepancies in scoring between pathologists were jointly reviewed, and a concordance was reached.

**2.4. Statistical Analysis.** All statistical analyses were executed using the SPSS statistical package for PC (version 14.0, IBM, Armonk, NY) as previously described [14, 15]. As a representation of indicative CSF-1 levels, tumors with scores of 1 or 2 were categorized as low expression (i.e., <50% positively stained cells), whereas tumors with scores of 3 or 4 were categorized as high expression (i.e., >50% positively stained cells). A Wilcoxon signed-rank test was used to test the difference of the CSF-1 expression between UTUC and the tumor-adjacent normal urothelium. Fisher’s and chi-square tests were used to analyze for associations between the CSF-1 expression and tumor size, tumor stage, tumor grade, gender, age, tumor side, lymphovascular invasion, distant metastasis, recurrence, and serum creatinine level. Survival curves were created using Kaplan-Meier estimates, and the importance of differences between curves was estimated using the log-rank test. In addition, hazard ratios (HRs) and 95% confidence intervals (CIs) calculated from univariate and multivariate Cox regression models were used to investigate the connection between clinicopathologic parameters and survival as previously described [14, 15]. *P* values less than 0.05 were regarded as statistically significant.

**2.5. Cell Lines and Cell Culture.** BFTC909, a human renal pelvis transitional cell line [30], was purchased from the Bioresource Collection and Research Center (BCRC, #60069, Taiwan). This cell line was cultured in Dulbecco’s Modified Eagle Medium (DMEM) supplemented with 10% fetal bovine serum (FBS) and antibiotic-antimycotic (Gibco™) and incubated at 37°C, 5% CO<sub>2</sub>. UM-UC-14, a human transitional cell carcinoma of the renal pelvis, was purchased from the European Collection of Authenticated Cell Cultures

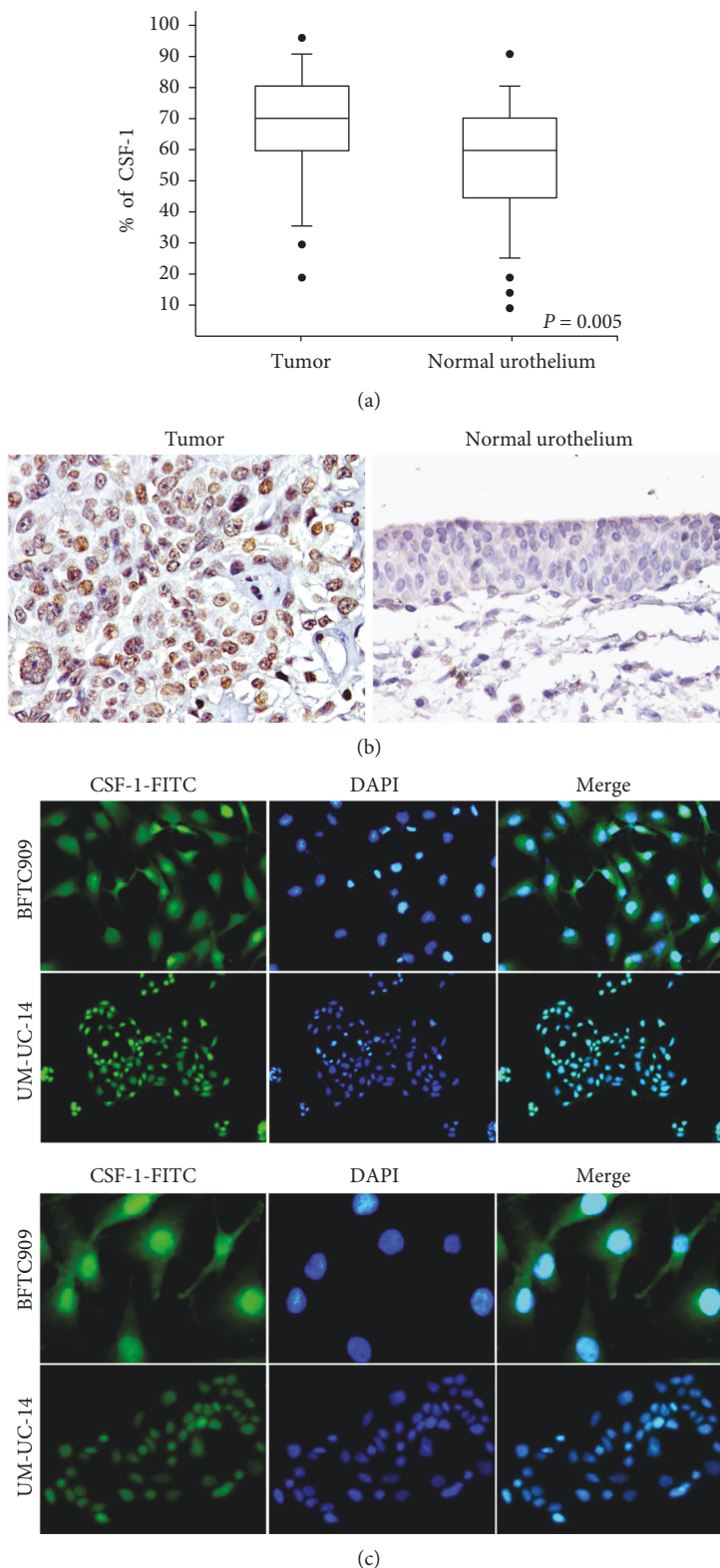


FIGURE 1: (a) Comparison with CSF-1 levels in 35 pairs of upper tract urothelial carcinomas (UTUC) and the corresponding cancer-adjacent normal tissues. The CSF-1 expression level was significantly higher in UTUC than in the normal urothelium (paired Wilcoxon signed-rank test,  $P = 0.005$ ). (b) Immunohistochemistry staining for CSF-1 in UTUC and normal urothelium. ( $\times 200$ ). (c) CSF-1 mainly localized in the nucleus of BFTC909 and UM-UC-14 cancer cells. Analysis of CSF-1 intracellular localization by immunofluorescence. Routinely cultured cells were subjected to immunofluorescence using an anti-CSF-1 antibody and nucleus stained with the DAPI. (upper panels:  $\times 400$ , lower panels:  $\times 200$ ).

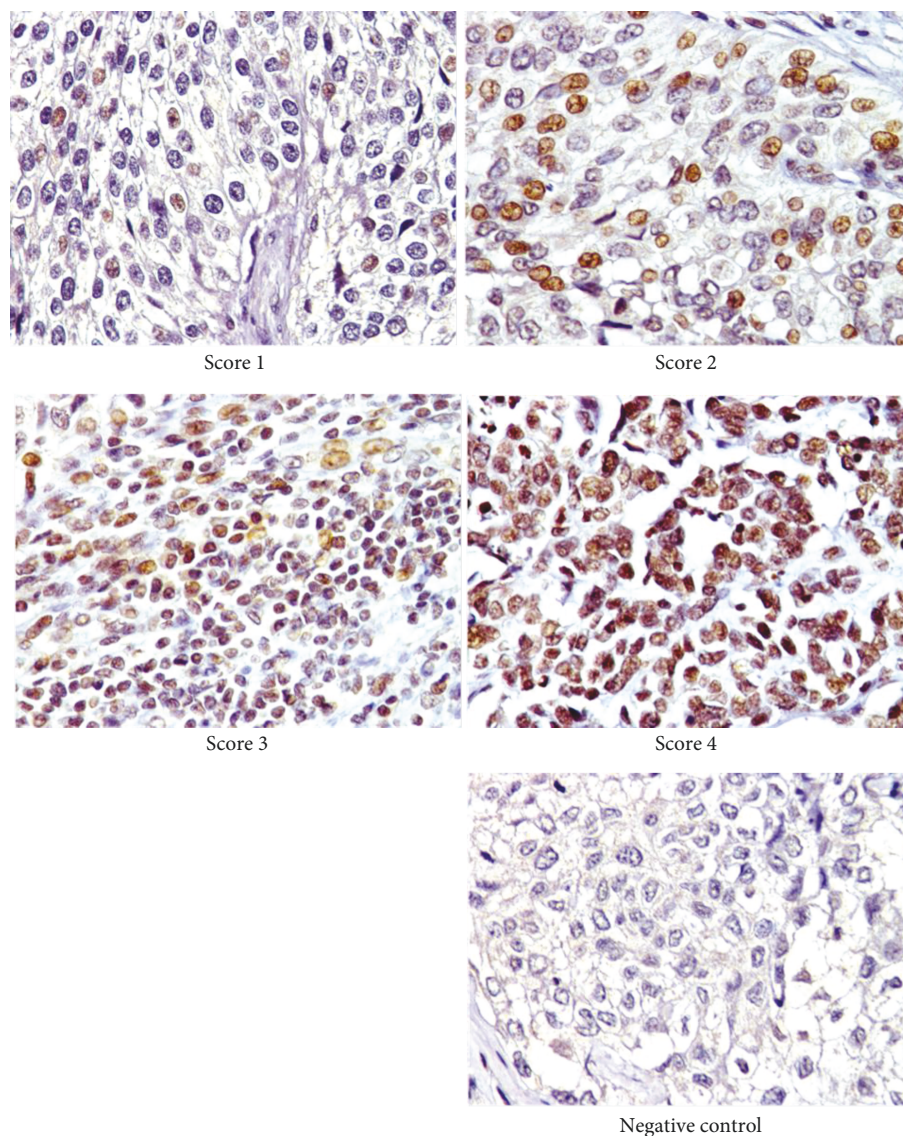


FIGURE 2: The expression of CSF-1 in UTUC tissue was analyzed by immunohistochemistry. The extent of the expression was partitioned into four classifications: score 1, <25% positive staining of tumor cells; score 2, 26% to 50% positive staining of tumor cells; score 3, 51% to 75% positive staining of tumor cells; and score 4, >76% positive staining of tumor cells ( $\times 200$ ).

(ECACC). This cell line was cultured in Eagle's Minimum Essential Medium (EMEM) supplemented with 10% FBS, 2 mM glutamine, 1% nonessential amino acids (NEAA), and antibiotic-antimycotic and incubated at 37°C, 5% CO<sub>2</sub>.

**2.6. Immunofluorescence.** BFTC909 and UM-UC-14 cell lines were seeded in a 35 mm Glass Bottom Dish (ibidi) and incubated at 37°C, 5% CO<sub>2</sub>. Immunofluorescence was performed using the Image-iT™ Fixation/Permeabilization Kit (Invitrogen™). We removed the culture medium from the cells and then performed cell fixation, permeabilization, and a blocking procedure per the manufacturer's protocol. After blocking, we aspirated the blocking solution and incubated the cells with an anti-CSF-1 monoclonal antibody (M-CSF Antibody (D-4), sc-365779, Santa Cruz) at a 1:50 dilution in blocking solution at 4°C overnight. The cells were then incubated with fluorescein isothiocyanate- (FITC-) conjugated

secondary antibody diluted in phosphate-buffered saline (PBS) for 1 h at room temperature (protected from light). Next, the cells were incubated with DAPI (Thermo Scientific™) diluted in PBS for 10 min at room temperature in the dark. Finally, cells were mounted by ProLong™ Gold Antifade Mountant (Thermo Scientific™) and observed using a fluorescence microscope.

### 3. Results

**3.1. CSF-1 Expression in Human UTUC and Nontumor Urothelial Tissues.** To validate the CSF-1 expression, we investigated UTUC tissue samples from 35 patients compared to paired cancer-adjacent normal tissues by immunohistochemistry. We found that the CSF-1 expression was significantly higher in UTUC tissues than in the noncancerous urothelium ( $P = 0.005$ ) (Figure 1(a)). Positive staining



TABLE 1: Correlation of CSF-1 expression with clinicopathological characteristics in upper tract urothelial carcinomas.

Variables	Item	Patient no. (%)	CSF-1				P value
			Low		High		
			No.	%	No.	%	
Total		112 (100)	58	51.8	54	48.2	
Stage	I/II	73 (65.2)	47	81.0	26	48.1	<0.001 <sup>a</sup>
	III/IV	39 (34.8)	11	19.0	28	51.9	
Grade	Low	30 (26.8)	17	29.3	13	24.1	0.532 <sup>a</sup>
	High	82 (73.2)	41	70.7	41	75.9	
Gender	Female	68 (60.7)	37	63.8	31	57.4	0.489 <sup>a</sup>
	Male	44 (39.3)	21	36.2	23	42.6	
Age (years)	<65	42 (37.5)	17	29.3	25	46.3	0.068 <sup>a</sup>
	≥65	70 (62.5)	41	70.7	29	53.7	
Tumor location	Ureter	47 (42.0)	25	43.1	22	40.7	0.300 <sup>a</sup>
	Renal pelvis	45 (40.2)	20	34.5	25	46.3	
	Renal pelvis+ureter	20 (17.9)	13	22.4	7	13.0	
Tumor side <sup>c</sup>	Right	49 (44.5)	25	44.6	24	44.4	0.983 <sup>a</sup>
	Left	61 (55.5)	31	55.4	30	55.6	
Lymphovascular invasion	Negative	89 (79.5)	48	82.8	41	75.9	0.371 <sup>a</sup>
	Positive	23 (20.5)	10	17.2	13	24.1	
Distant metastasis	Negative	96 (85.7)	55	94.8	41	75.9	0.006 <sup>b</sup>
	Positive	16 (14.3)	3	5.2	13	24.1	
Recurrence	Negative	62 (55.4)	40	69.0	22	40.7	0.003 <sup>a</sup>
	Positive	50 (44.6)	18	31.0	32	59.3	
Cancer death	No	93 (83.0)	54	93.1	39	72.2	0.005 <sup>b</sup>
	Yes	19 (17.0)	4	6.9	15	27.8	
Creatinine (mg/dl)	≤1.5	66 (58.9)	35	60.3	31	57.4	0.752 <sup>a</sup>
	>1.5	46 (41.1)	23	39.7	23	42.6	

<sup>a</sup>The *P* value was calculated by the chi-square test. <sup>b</sup>The *P* value was calculated by the Fisher's exact test. <sup>c</sup>Tumor side was not determined in a small portion of the patients.

expression of CSF-1 predominantly appeared in the nucleus of tumor cells in UTUC tissues (Figure 1(b)). We also used the immunofluorescence method to detect the CSF-1 location in UTUC cell lines (BFTC909 and UM-UC-14). The results revealed that CSF-1 was confined to the cytoplasm and nucleus, and it demonstrated a significantly higher expression in the nucleus than in the cytoplasm (Figure 1(c)).

**3.2. Association between CSF-1 Expression and Patient Characteristics.** The expression of CSF-1 in UTUC tissues ( $n = 112$ ) was examined by immunohistochemistry and categorized into four scores (quartiles). On the basis of the scoring, tumor tissues were further sorted into low (scores of 1 and 2; 51.8%) and high (scores of 3 and 4; 48.2%) CSF-1 expression groups (Figure 2 and Table 1). We found that the CSF-1 expression was positively correlated with tumor size ( $P = 0.04$ , data not shown). Next, we examined the CSF-1 expression for indication of correlation with different clinicopathologic characteristics including tumor stage, grade, gender, age, tumor location, tumor side, lymphovascular invasion, distant metastasis, recurrence, cancer death, and serum creatinine level. The correlations between these clinicopathologic variables and CSF-1 expression are listed

in Table 1. We found that high CSF-1 expression in UTUC tissues was significantly associated with tumor stage ( $P < 0.001$ ), distant metastasis ( $P = 0.006$ ), recurrence ( $P = 0.003$ ), and cancer death ( $P = 0.005$ ).

**3.3. A High Expression of CSF-1 Is Correlated with Poor Prognosis.** To examine parameters related to CSF-1 expression in UTUC patients, we used univariate and multivariate analyses. The data indicated significant associations between disease-free survival and the following two factors: tumor stage (HR = 1.76, CI = 1.01-3.08,  $P = 0.046$ ) and CSF-1 expression (HR = 2.14, CI = 1.20-3.81,  $P = 0.01$ ) in univariate analysis (Table 2). However, following the multivariate analysis, only the CSF-1 expression was related to disease-free survival (HR = 2.56, CI = 1.30-5.04,  $P = 0.007$ ) (Table 2). Univariate analysis also demonstrated that both tumor stage and CSF-1 expression were associated with cancer-specific survival (Table 2). High tumor stage and CSF-1 expression were correlated with a significant reduction in cancer-specific survival (HR = 6.03, CI = 2.17-16.80,  $P = 0.001$ , and HR = 5.18, CI = 1.71-15.71,  $P = 0.004$ , respectively). In the multivariate analysis, we found that cancer-specific survival was also related to CSF-1 expression (HR = 5.14,

TABLE 2: Univariate and multivariate analyses of disease-free survival and cancer-specific survival for upper tract urothelial carcinomas.

Variables	Item	Disease-free survival						Cancer-specific survival					
		Univariate			Multivariate			Univariate			Multivariate		
		HR	95% CI	P value	HR	95% CI	P value	HR	95% CI	P value	HR	95% CI	P value
Stage	III/IV	1.76	1.01-3.08	0.046	1.18	0.57-2.44	0.661	6.03	2.17-16.80	0.001	4.18	1.00-17.51	0.051
	I/II	1.00			1.00			1.00			1.00		
Grade	High	1.15	0.61-2.17	0.659	1.05	0.50-2.22	0.902	1.65	0.55-4.99	0.376	0.63	0.14-2.86	0.547
	Low	1.00			1.00			1.00			1.00		
Gender	Male	1.24	0.71-2.16	0.456	1.18	0.64-2.16	0.596	1.36	0.55-3.36	0.501	0.89	0.32-2.43	0.815
	Female	1.00			1.00			1.00			1.00		
Age (years)	≥65	1.68	0.92-3.05	0.091	1.54	0.78-3.07	0.216	1.43	0.54-3.77	0.470	1.11	0.33-3.72	0.870
	<65	1.00			1.00			1.00			1.00		
Tumor location	Renal pelvis + ureter	1.39	0.68-2.83	0.364	1.47	0.64-3.37	0.365	1.11	0.37-3.32	0.856	1.33	0.31-5.82	0.701
	Renal pelvis	0.76	0.40-1.45	0.406	0.67	0.34-1.31	0.243	0.56	0.19-1.68	0.301	0.42	0.13-1.34	0.143
	Ureter	1.00			1.00			1.00			1.00		
Tumor side	Left	0.80	0.46-1.40	0.443	0.84	0.46-1.55	0.584	0.59	0.24-1.48	0.263	0.43	0.14-1.29	0.131
	Right	1.00			1.00			1.00			1.00		
Lymphovascular invasion	Positive	1.35	0.72-2.55	0.351	1.13	0.54-2.39	0.745	2.49	0.97-6.34	0.057	2.15	0.69-6.70	0.186
	Negative	1.00			1.00			1.00			1.00		
Creatinine (mg/dl)	>1.5	1.06	0.60-1.88	0.844	0.93	0.50-1.73	0.822	0.76	0.29-2.00	0.570	0.59	0.19-1.76	0.342
	≤1.5	1.00			1.00			1.00			1.00		
CSF-1	High	2.14	1.20-3.81	0.010	2.56	1.30-5.04	0.007	5.18	1.71-15.71	0.004	5.14	1.27-20.84	0.022
	Low	1.00			1.00			1.00			1.00		

Abbreviations: HR: hazard ratio; CI: confidence interval.

CI = 1.27-20.84,  $P = 0.022$ ). Next, we explored whether the CSF-1 expression in human UTUC tissue samples was correlated to disease-free survival and cancer-specific survival of patients using Kaplan-Meier survival analysis. Kaplan-Meier survival curves showed that higher CSF-1 expression correlated with a significantly lower disease-free survival ( $P = 0.008$ ) and cancer-specific survival ( $P = 0.001$ ) (Figure 3).

#### 4. Discussion

We offered the first evidence that high CSF-1 expression is a potential prognostic marker for predicting patient survival and recurrence of UTUC. First, the expression of CSF-1 was higher in UTUC tissues than in cancer-adjacent normal tissues. Second, positive staining of CSF-1 was mainly expressed in the nucleus. Third, a high level of CSF-1 positively correlated with tumor stage, tumor size, distant metastasis, and recurrence. Finally, CSF-1 expression was associated with poor disease-free and cancer-specific survival, and univariate and multivariate proportional hazard analyses indicated that it was also an independent prognostic biomarker for patients with UTUC.

CSF-1 is a cytokine generated by different types of cells, and it regulates the biological functions of monocytes and macrophages, including cell proliferation, differentiation, and survival [16, 17, 31]. Moreover, CSF-1 has also been reported to induce angiogenic activity via recruitment of macrophages, which secrete growth factors, proangiogenic cytokines, and matrix metalloproteases (MMPs) to regulate

tumor cell invasion [32]. CSF-1 interacts with CSF-1R, which is a tyrosine kinase transmembrane receptor produced by the *c-fms* protooncogene [33]. The CSF-1/CSF-1R axis has an important role in inflammation and immunity [31]. Moreover, CSF-1 and CSF-1R are also expressed in tumor-associated macrophages (TAMs), promoting tumor progression and metastasis in several cancers [18, 34]. Studies have shown that a paracrine loop in CSF-1/CSF-1R signaling between TAMs and tumor cells is required in the tumor microenvironment. Consistent with these findings, our results demonstrated that high expression of CSF-1 in UTUC tissue was correlated with tumor stage and distant metastasis. Furthermore, recent findings indicate that CSF-1 signal transduction pathways have an autocrine-loop function in cancer cells. For instance, the CSF-1/CSF-1R axis could induce phosphorylation and activation of STAT3, which promotes cell survival and proliferation in renal cell carcinoma [35]. Interestingly, our previous studies demonstrated that high activated phospho-STAT3 (Ser727) expression is associated with advanced tumor stage in UTUC tissues and can predict poor prognosis in advanced-stage UTUC patients [15]. STAT3 is a transcription factor whose activation contributes to many cancer functions including survival, proliferation, inflammation, angiogenesis, invasion, and metastasis and is regarded as an oncogene [36-38]. Importantly, STAT3 activation has also been found to contribute to the immunosuppressive tumor microenvironment by prohibiting tumor cell apoptosis and promoting tumor growth and metastasis [39]. Based on the conjunction of

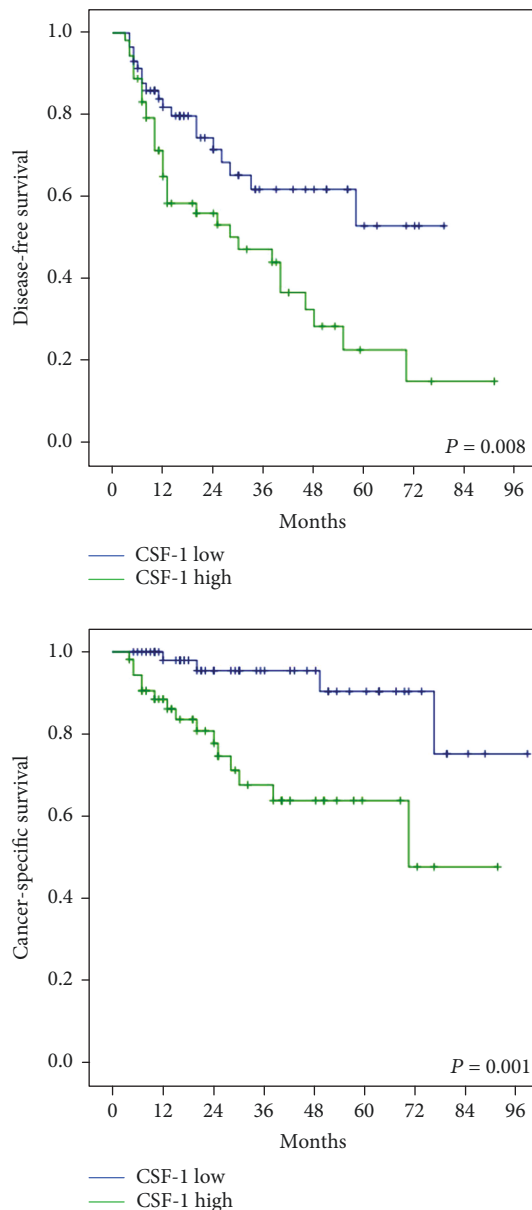


FIGURE 3: Kaplan-Meier survival curves for disease-free survival and cancer-specific survival rates of patients with CSF-1 expression in upper tract urothelial carcinomas.

previous findings and our studies, we hypothesized that the CSF-1 signaling pathway may be involved in UTUC development by regulating phospho-STAT3 expression. It will be taken into consideration in our future studies.

In this study, the immunohistochemistry analysis revealed that the staining of CSF-1 was primarily expressed in the nucleus, although previous studies indicated the staining position of CSF-1 was also in the cytoplasm of various cancer cells such as renal cell carcinoma, soft tissue sarcomas, and gastric cancer [29, 40, 41]. CSF-1 that is located in the nucleus has been aptly named “nuclear-presenting M-CSF” (nM-CSF) [42, 43]. CSF-1 can also colocalize with CSF-1R in the nucleus in breast cancer cells [44]. Nuclear-presenting M-CSF has been shown to promote cancer cell proliferation and migration [45]. Our immunofluorescence staining in

UTUC cancer cells also found CSF-1 to be prominently expressed in the nucleus. The evidence of these studies and our results suggest that CSF-1 expressed in the nucleus may contribute to UTUC progression and metastasis. However, the specific molecular mechanisms of CSF-1 in the nucleus of UTUC cells is not widely understood. Although there was a significant correlation between CSF-1 expression and poor prognosis in this study, the sample size was small; a multi-institutional study with a more substantial sample size is required to verify our results. Finally, we hope our results can help with a prognostic determination for UTUC patients and also help indicate a potential plan for aggressive treatment.

## 5. Conclusions

High CSF-1 expression was found to be an independent predictor of poor survival rates in patients with UTUC. We hope our results will help determine the prognosis for UTUC patients and may also help indicate a plan for aggressive treatment.

## Data Availability

The data used to support the findings of this study are included within the article.

## Conflicts of Interest

To the best of our knowledge, the named authors have no conflict of interest, financial or otherwise.

## Acknowledgments

This study was supported by grants from the Ministry of Science and Technology (MOST107-2314-B-037-011) and Kaohsiung Medical University Hospital (KMUH-103-3T11, KMUH-104-4R43, and KMUH-105-5R70).

## References

- [1] M. Pérez-Utrilla Pérez, A. Aguilera Bazán, J. M. Alonso Dorrego, R. Vitón Herrero, J. Cisneros Ledo, and J. de la Peña Barthel, “Simultaneous cystectomy and nephroureterectomy due to synchronous upper urinary tract tumors and invasive bladder cancer: open and laparoscopic approaches,” *Current Urology*, vol. 6, no. 2, pp. 76–81, 2012.
- [2] M. Rouprêt, M. Babjuk, E. Compérat et al., “European guidelines on upper tract urothelial carcinomas: 2013 update,” *European Urology*, vol. 63, no. 6, pp. 1059–1071, 2013.
- [3] Y. H. Chou and C. H. Huang, “Unusual clinical presentation of upper urothelial carcinoma in Taiwan,” *Cancer*, vol. 85, no. 6, pp. 1342–1344, 1999.
- [4] M. I. Fernández, S. F. Shariat, V. Margulis et al., “Evidence-based sex-related outcomes after radical nephroureterectomy for upper tract urothelial carcinoma: results of large multicenter study,” *Urology*, vol. 73, no. 1, pp. 142–146, 2009.
- [5] J. Ferlay, E. Steliarova-Foucher, J. Lortet-Tieulent et al., “Cancer incidence and mortality patterns in Europe: estimates for 40 countries in 2012,” *European Journal of Cancer*, vol. 49, no. 6, pp. 1374–1403, 2013.

- [6] J. J. Munoz and L. M. Ellison, "Upper tract urothelial neoplasms: incidence and survival during the last 2 decades," *The Journal of Urology*, vol. 164, no. 5, pp. 1523–1525, 2000.
- [7] R. L. Siegel, K. D. Miller, and A. Jemal, "Cancer statistics, 2016," *CA: A Cancer Journal for Clinicians*, vol. 66, no. 1, pp. 7–30, 2016.
- [8] M. Bianconi, A. Cimadamore, L. Faloppi et al., "Contemporary best practice in the management of urothelial carcinomas of the renal pelvis and ureter," *Therapeutic Advances in Urology*, vol. 11, article 1756287218815372, 2019.
- [9] M. H. Yang, K. K. Chen, C. C. Yen et al., "Unusually high incidence of upper urinary tract urothelial carcinoma in Taiwan," *Urology*, vol. 59, no. 5, pp. 681–687, 2002.
- [10] V. Stefanovic and Z. Radovanovic, "Balkan endemic nephropathy and associated urothelial cancer," *Nature Clinical Practice Urology*, vol. 5, no. 2, pp. 105–112, 2008.
- [11] A. P. Grollman, "Aristolochic acid nephropathy: harbinger of a global iatrogenic disease," *Environmental and Molecular Mutagenesis*, vol. 54, no. 1, pp. 1–7, 2013.
- [12] E. Mearini, G. Poli, G. Cochetti, A. Boni, M. G. Egidi, and S. Brancorsini, "Expression of urinary miRNAs targeting NLRs inflammasomes in bladder cancer," *OncoTargets and Therapy*, vol. 10, pp. 2665–2673, 2017.
- [13] H. L. Ke, Y. C. Wei, S. F. Yang et al., "Overexpression of hypoxia-inducible factor-1 $\alpha$  predicts an unfavorable outcome in urothelial carcinoma of the upper urinary tract," *International Journal of Urology*, vol. 15, no. 3, pp. 200–205, 2008.
- [14] Y. C. Lee, W. J. Wu, H. H. Lin et al., "Prognostic value of leptin receptor overexpression in upper tract urothelial carcinomas in Taiwan," *Clinical Genitourinary Cancer*, vol. 15, no. 4, pp. e653–e659, 2017.
- [15] W. M. Li, C. N. Huang, Y. C. Lee et al., "Over-expression of activated signal transducer and activator of transcription 3 predicts poor prognosis in upper tract urothelial carcinoma," *International Journal of Medical Sciences*, vol. 14, no. 13, pp. 1360–1367, 2017.
- [16] F. J. Pixley and E. R. Stanley, "CSF-1 regulation of the wandering macrophage: complexity in action," *Trends in Cell Biology*, vol. 14, no. 11, pp. 628–638, 2004.
- [17] W. Yu, J. Chen, Y. Xiong, F. J. Pixley, Y. G. Yeung, and E. R. Stanley, "Macrophage proliferation is regulated through CSF-1 receptor tyrosines 544, 559, and 807," *Journal of Biological Chemistry*, vol. 287, no. 17, pp. 13694–13704, 2012.
- [18] E. Y. Lin, A. V. Nguyen, R. G. Russell, and J. W. Pollard, "Colony-stimulating factor 1 promotes progression of mammary tumors to malignancy," *The Journal of Experimental Medicine*, vol. 193, no. 6, pp. 727–740, 2001.
- [19] S. Goswami, E. Sahai, J. B. Wyckoff et al., "Macrophages promote the invasion of breast carcinoma cells via a colony-stimulating factor-1/epidermal growth factor paracrine loop," *Cancer Research*, vol. 65, no. 12, pp. 5278–5283, 2005.
- [20] E. P. Toy, M. Azodi, N. L. Folk, C. M. Zito, C. J. Zeiss, and S. K. Chambers, "Enhanced ovarian cancer tumorigenesis and metastasis by the macrophage colony-stimulating factor," *Neoplasia*, vol. 11, no. 2, pp. 136–144, 2009.
- [21] S. K. Chambers, "Role of CSF-1 in progression of epithelial ovarian cancer," *Future Oncology*, vol. 5, no. 9, pp. 1429–1440, 2009.
- [22] S. Ramakrishnan, F. J. Xu, S. J. Brandt, J. E. Niedel, R. C. Bast Jr., and E. L. Brown, "Constitutive production of macrophage colony-stimulating factor by human ovarian and breast cancer cell lines," *The Journal of Clinical Investigation*, vol. 83, no. 3, pp. 921–926, 1989.
- [23] B. M. Kacinski, K. A. Scata, D. Carter et al., "FMS (CSF-1 receptor) and CSF-1 transcripts and protein are expressed by human breast carcinomas *in vivo* and *in vitro*," *Oncogene*, vol. 6, no. 6, pp. 941–952, 1991.
- [24] C. L. Behnes, F. Bremmer, B. Hemmerlein, A. Strauss, P. Ströbel, and H. J. Radzun, "Tumor-associated macrophages are involved in tumor progression in papillary renal cell carcinoma," *Virchows Archiv*, vol. 464, no. 2, pp. 191–196, 2014.
- [25] B. M. Kacinski, D. Carter, K. Mittal et al., "Ovarian adenocarcinomas express fms-complementary transcripts and fms antigen, often with coexpression of CSF-1," *The American Journal of Pathology*, vol. 137, no. 1, pp. 135–147, 1990.
- [26] M. Groblewska, B. Mroczko, U. Wereszczyńska-Siemiakowska, P. Myśliwiec, B. Kedra, and M. Szmitkowski, "Serum levels of granulocyte colony-stimulating factor (G-CSF) and macrophage colony-stimulating factor (M-CSF) in pancreatic cancer patients," *Clinical Chemistry and Laboratory Medicine*, vol. 45, no. 1, pp. 30–34, 2007.
- [27] R. S. McDermott, L. Deneux, V. Mosseri et al., "Circulating macrophage colony stimulating factor as a marker of tumour progression," *European Cytokine Network*, vol. 13, no. 1, pp. 121–127, 2002.
- [28] B. Mroczko, M. Groblewska, U. Wereszczyńska-Siemiakowska et al., "Serum macrophage-colony stimulating factor levels in colorectal cancer patients correlate with lymph node metastasis and poor prognosis," *Clinica Chimica Acta*, vol. 380, no. 1-2, pp. 208–212, 2007.
- [29] L. Yang, Q. Wu, L. Xu et al., "Increased expression of colony stimulating factor-1 is a predictor of poor prognosis in patients with clear-cell renal cell carcinoma," *BMC Cancer*, vol. 15, no. 1, p. 67, 2015.
- [30] C. C. Tzeng, H.-S. Liu, C. Li et al., "Characterization of two urothelium cancer cell lines derived from a blackfoot disease endemic area in Taiwan," *Anticancer Research*, vol. 16, no. 4A, pp. 1797–1804, 1996.
- [31] V. Chitu and E. R. Stanley, "Colony-stimulating factor-1 in immunity and inflammation," *Current Opinion in Immunology*, vol. 18, no. 1, pp. 39–48, 2006.
- [32] S. Aharinejad, P. Paulus, M. Sioud et al., "Colony-stimulating factor-1 blockade by antisense oligonucleotides and small interfering RNAs suppresses growth of human mammary tumor xenografts in mice," *Cancer Research*, vol. 64, no. 15, pp. 5378–5384, 2004.
- [33] C. J. Sherr, C. W. Rettenmier, R. Sacca, M. F. Roussel, A. T. Look, and E. R. Stanley, "The c-fms proto-oncogene product is related to the receptor for the mononuclear phagocyte growth factor, CSF-1," *Cell*, vol. 41, no. 3, pp. 665–676, 1985.
- [34] J. Wyckoff, W. Wang, E. Y. Lin et al., "A paracrine loop between tumor cells and macrophages is required for tumor cell migration in mammary tumors," *Cancer Research*, vol. 64, no. 19, pp. 7022–7029, 2004.
- [35] Y. Komohara, H. Hasita, K. Ohnishi et al., "Macrophage infiltration and its prognostic relevance in clear cell renal cell carcinoma," *Cancer Science*, vol. 102, no. 7, pp. 1424–1431, 2011.
- [36] J. F. Bromberg, M. H. Wrzeszczynska, G. Devgan et al., "Stat3 as an oncogene," *Cell*, vol. 98, no. 3, pp. 295–303, 1999.
- [37] K. S. Siveen, S. Sikka, R. Surana et al., "Targeting the STAT3 signaling pathway in cancer: role of synthetic and natural



- inhibitors,” *Biochimica et Biophysica Acta (BBA) - Reviews on Cancer*, vol. 1845, no. 2, pp. 136–154, 2014.
- [38] L. Avalle, A. Camporeale, A. Camperi, and V. Poli, “STAT3 in cancer: a double edged sword,” *Cytokine*, vol. 98, pp. 42–50, 2017.
- [39] H. Yu, M. Kortylewski, and D. Pardoll, “Crosstalk between cancer and immune cells: role of STAT3 in the tumour micro-environment,” *Nature Reviews Immunology*, vol. 7, no. 1, pp. 41–51, 2007.
- [40] E. Richardson, S. W. Sørbye, J. P. Crowe, J.-L. Yang, and L.-T. Busund, “Expression of M-CSF and CSF-1R is correlated with histological grade in soft tissue tumors,” *Anticancer Research*, vol. 29, no. 10, pp. 3861–3866, 2009.
- [41] H. Liu, H. Zhang, Z. Shen et al., “Increased expression of CSF-1 associates with poor prognosis of patients with gastric cancer undergoing gastrectomy,” *Medicine*, vol. 95, no. 9, article e2675, 2016.
- [42] S. M. Scholl, C. Pallud, F. Beuvon et al., “Anti-colony-stimulating factor-1 antibody staining in primary breast adenocarcinomas correlates with marked inflammatory cell infiltrates and prognosis,” *Journal of the National Cancer Institute*, vol. 86, no. 2, pp. 120–126, 1994.
- [43] S. S. Tang, G. G. Zheng, K. F. Wu, G. B. Chen, H. Z. Liu, and Q. Rao, “Autocrine and possible intracrine regulation of HL-60 cell proliferation by macrophage colony-stimulating factor,” *Leukemia Research*, vol. 25, no. 12, pp. 1107–1114, 2001.
- [44] V. Barbetti, A. Morandi, I. Tusa et al., “Chromatin-associated CSF-1R binds to the promoter of proliferation-related genes in breast cancer cells,” *Oncogene*, vol. 33, no. 34, pp. 4359–4364, 2014.
- [45] Z. Y. Cao, B. Zhang, Q. Rao, G. Li, G. G. Zheng, and K. F. Wu, “Effects of nuclear-presenting-macrophage colony-stimulating factor on the process of malignancy,” *International Journal of Hematology*, vol. 78, no. 1, pp. 87–89, 2003.

## Research Article

# The Prognostic Significance of Protein Expression of CASZ1 in Clear Cell Renal Cell Carcinoma

Bohyun Kim , Minsun Jung, and Kyung Chul Moon 

Department of Pathology, Seoul National University College of Medicine, Republic of Korea

Correspondence should be addressed to Kyung Chul Moon; [blue7270@snu.ac.kr](mailto:blue7270@snu.ac.kr)

Received 9 May 2019; Revised 11 July 2019; Accepted 17 July 2019; Published 6 August 2019

Guest Editor: Oommen P. Oommen

Copyright © 2019 Bohyun Kim et al. This is an open access article distributed under the Creative Commons Attribution License, which permits unrestricted use, distribution, and reproduction in any medium, provided the original work is properly cited.

**Backgrounds.** Clear cell renal cell carcinoma (ccRCC) is the most common histologic subtype of renal cell carcinoma (RCC) and shows a relatively poor prognosis among RCCs. Castor zinc finger 1 (CASZ1) is a transcription factor, prominently known for its tumor suppression role in neuroblastoma and other cancers. However, there has been no research about the prognostic significance of CASZ1 in ccRCC. In this study, we investigated CASZ1 expression in ccRCC and analyzed its prognostic implications. **Methods.** A total of 896 ccRCC patients, who underwent surgical resection from 1995 to 2008, were included. We prepared tissue microarray blocks, evaluated CASZ1 nuclear expression by immunohistochemistry, and classified the cases into low or high expression categories. **Results.** A low expression of CASZ1 was observed in 320 cases (35.7%) and was significantly associated with large tumor size, high World Health Organization/International Society of Urological Pathology (WHO/ISUP) grade, and high T category and M category. In survival analysis, a low expression of CASZ1 was significantly correlated with unfavorable progression-free survival (PFS) ( $p < 0.001$ ), overall survival (OS) ( $p < 0.001$ ), and cancer-specific survival (CSS) ( $p < 0.001$ ) and was an independent prognostic factor for PFS and CSS in multivariate analysis adjusted for tumor size, WHO/ISUP grade, T category, N category, and M category. **Conclusions.** Our study is the first to show the prognostic significance of CASZ1 expression in ccRCC. Our results revealed that low expression of CASZ1 is associated with poor prognosis and may serve as a new prognostic indicator.

## 1. Introduction

Kidney cancer is the 15th most common cancer and the 17th most common cause of cancer-related death worldwide [1]. Renal cell carcinoma (RCC) is the most common malignant kidney tumor [2], and its incidence is increasing [3]. RCC is a heterogeneous group of carcinomas that includes a clear cell subtype, a papillary subtype, and a chromophobe subtype [4]. Each subtype differs in histological characteristics, aggressiveness, and prognosis [5]. The most common histological subtype is the clear cell type, which makes up 80% of all RCCs [6]. For clear cell RCC (ccRCC), surgical excision is the primary treatment option, and in cases of surgically unresectable tumors or in cases of recurrence, pazopanib or sunitinib is used as first-line therapy [7].

Castor zinc finger 1 (CASZ1) is a transcription factor that has been reported to play an important role in neural and cardiac development [8, 9]. Some studies have suggested

that CASZ1 induces vascular assembly and morphogenesis [10, 11]. Recent studies reported that CASZ1 regulates T helper cell plasticity and has important implications for autoimmune inflammation [12]. Some studies showed that CASZ1 has a role in tumor progression. CASZ1 regulates tumor growth and the process of development and thus can be a candidate for tumor suppression in neuroblastomas [13, 14]. Additionally, loss of CASZ1 is associated with poor prognosis in neuroblastomas [15]. CASZ1 was found to be significantly hypermethylated in esophageal squamous cell carcinoma [16]. A CASZ1-MASP2 fusion transcript was identified in colorectal cancer with 3' overexpression of MASP2 [17]. CASZ1 downregulation was correlated with aggressiveness and poor outcome in hepatocellular carcinoma (HCC) [18]. On the other hand, CASZ1 promoted the epithelial-mesenchymal transition and cancer metastasis in epithelial ovary cancer [19]. CASZ1 possibly plays different roles in various cancers. It has been reported that the

expression of CASZ1 is downregulated in ccRCC tissue [13], but no study so far has investigated the relationship between CASZ1 expression and prognosis in ccRCC. Thus, in this study, we investigated CASZ1 expression in ccRCC and analyzed its prognostic value.

## 2. Materials and Methods

**2.1. Patients and Tissue Samples.** In total, ccRCC tissues from 896 patients who underwent surgical resection at Seoul National University Hospital (SNUH) from 1995 to 2008 were included in this study. We searched the computerized database of the Department of Pathology, SNUH, and we retrospectively collected clinical and pathologic information from medical records and pathologic reports. We reviewed hematoxylin and eosin- (H&E-) stained slides to confirm the diagnosis and to identify various pathologic parameters.

A tissue microarray (TMA) block was prepared from formalin-fixed paraffin-embedded tissue blocks (SuperBio-Chips Laboratories, Seoul, Republic of Korea). For each case, two tumor cores (2 mm in diameter) were collected. Each core was derived from different tumor areas with representative clear cell histology.

This study was approved by the Institutional Review Board (IRB) of SNUH (IRB No H-1903-149-1022) and was performed in accordance with the principles of the Declaration of Helsinki.

**2.2. Immunohistochemistry (IHC).** For immunohistochemical analyses, the TMA blocks were cut at 4  $\mu$ m thickness. A rabbit anti-CASZ1 polyclonal antibody (Novus Biologicals, Centennial, CO, USA) was used at a dilution of 1 : 100. IHC was performed using the Ventana Benchmark XT automated staining system (Ventana Medical Systems, Tucson, AZ, USA) according to the manufacturer's instructions.

**2.3. Immunohistochemical Scoring.** CASZ1 immunohistochemical staining was mainly localized in the nucleus in positive cases. CASZ1 protein expression was evaluated by the percentage of positively stained cells. The percentage of stained cells is the ratio of the number of tumor cells with positive CASZ1 staining to the total number of tumor cells in the TMA tumor core area. The percentage of stained cells was scored 0 to 5+ (0: no tumor cell staining, 1+: <1%, 2+: 1%-10%, 3+: 11%-33%, 4+: 34%-66%, and 5+: 67%-100%). For each case, both cores were evaluated, and the mean value was used for statistical analysis. In receiver operating curve analysis, we discerned the optimal cut-off value with the highest Youden index [20]. A score of 2.5 was used as a cut-off value to classify all cases as either high CASZ1 expression or low CASZ1 expression. Representative images of high and low CASZ1 expressions are shown in Figure 1. One pathologist (B.K.) evaluated CASZ1 staining at two different time points, without awareness of the previous results at the second evaluation. Any cases with discrepant results were reviewed together with another pathologist (K.C.M.) for final scoring.

**2.4. Statistical Analysis.** The follow-up period was the time between the surgery and the last follow-up. The progression-

free survival (PFS) period was defined as the time period between the time of surgery and the time of recurrence at the operation site, lymph node metastasis, distant metastasis, or death by clear cell renal cell carcinoma. The overall survival (OS) period was defined as the time period between the time of surgery and the time of death, or it was censored at the time of the last follow-up. The cancer-specific survival (CSS) period was defined as the time period between the time of surgery and the time of cancer-related death, or it was censored at the time of the last follow-up.

The association between CASZ1 expression and the patient's clinicopathologic characteristics was evaluated by the chi-squared test. The associations between CASZ1 expression and PFS, CSS, and OS were evaluated by the Kaplan-Meier method with the log-rank test. The significance of covariates was evaluated by the univariate Cox proportional hazards model. Multivariate analysis was performed with covariates which showed statistical significance on univariate analysis. Statistical analyses were performed using SPSS software (version 23; IBM, Armonk, NY, USA). Two-sided  $p$  values of <0.05 were considered to be statistically significant.

## 3. Results

**3.1. Clinicopathologic Characteristics of Patients.** Overall, 896 patients were included in this study, including 671 men and 225 women. The age of the patients ranged from 20 to 84 years, with the mean age of 56 years. The diameter of primary tumors ranged from 5 to 220 mm, with the mean diameter of 47 mm. Lymph node metastasis was found in 16 cases (1.8%), and distant metastasis was found in 68 cases (7.6%). According to the 8th edition of the TNM staging system of the AJCC [21], 607 patients were in stage I, 77 patients in stage II, 139 patients in stage III, and 73 patients in stage IV. According to the WHO/ISUP grading system [22], 53 cases were classified as grade 1, 406 cases as grade 2, 360 cases as grade 3, and 77 cases as grade 4. There was no case that underwent neoadjuvant therapy. Sixty-eight cases underwent adjuvant therapy, which included 57 cases with distant metastasis at the time of surgery and some cases with T category 4 or with lymph node metastasis. A high expression of CASZ1 was observed in 83.6% (749/896); a low expression of CASZ1 was observed in 16.4% (147/896).

**3.2. Association of CASZ1 Expression with Clinicopathologic Characteristics.** Table 1 summarizes the clinical and pathologic characteristics of the 896 cases. The low expression of CASZ1 was significantly correlated with old age (>55 years) ( $p = 0.037$ ), large tumor size ( $p = 0.004$ ), high WHO/ISUP grade ( $p < 0.001$ ), and high T category ( $p < 0.001$ ) and M category ( $p = 0.008$ ) but not correlated with gender or N category.

**3.3. Association of CASZ1 Expression with Prognosis.** The follow-up period ranged from 1 to 288 months, and the median follow-up period was 94 months. During the follow-up period, disease progression was found in 117 cases (13.1%) and cancer-related death occurred in 53 cases (5.9%). Kaplan-Meier analysis showed that the low

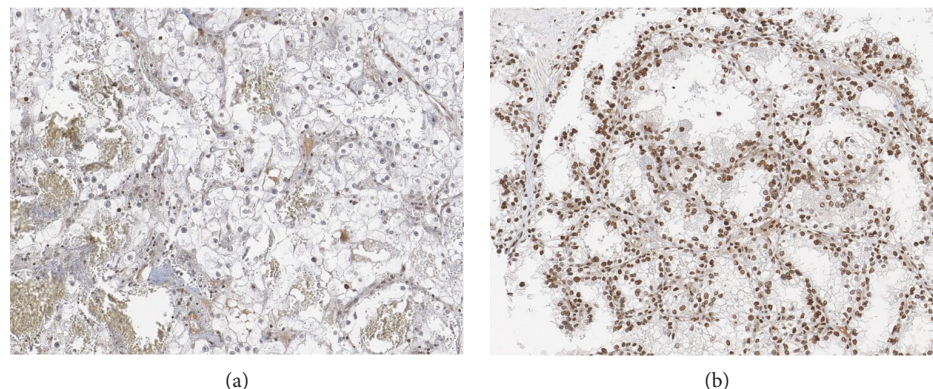


FIGURE 1: Immunohistochemical expression of CASZ1 in clear cell renal cell carcinoma. Representative images of low (a) and high (b) expressions ( $\times 200$ ).

TABLE 1: Clinicopathologic characteristics of patients and association with CASZ1 expression.

	CASZ1 expression		<i>p</i> value
	Low <i>N</i> (%)	High <i>N</i> (%)	
Age (years)			
≤55	58 (39.5%)	366 (48.9%)	0.037
>55	89 (60.5%)	383 (51.1%)	
Gender			
Male	111 (75.5%)	560 (74.8%)	0.849
Female	36 (24.5%)	189 (25.2%)	
Tumor size (cm)			
≤7	100 (68.0%)	592 (79.0%)	0.004
>7	47 (32.0%)	157 (21.0%)	
WHO/ISUP grade			
Grades 1-2	54 (36.7%)	405 (54.1%)	<0.001
Grades 3-4	93 (63.3%)	344 (45.9%)	
T category			
T1-T2	101 (68.7%)	619 (82.6%)	<0.001
T3-T4	46 (31.3%)	130 (17.4%)	
N category			
N0/Nx	143 (97.3%)	737 (98.4%)	0.349
N1	4 (2.7%)	12 (1.6%)	
M category			
M0	182 (87.1%)	700 (93.5%)	0.008
M1	19 (12.9%)	49 (6.5%)	

expression of CASZ1 was associated with unfavorable OS, CSS, and PFS ( $p < 0.001$ ,  $p < 0.001$ , and  $p < 0.001$ , respectively) (Figure 2).

**3.4. Univariate and Multivariate Analyses of Clinicopathologic Parameters and Expression of CASZ1.** Cox proportional hazards analysis was performed to analyze the risk factors associated with the survival of ccRCC patients. The results are summarized in Tables 2 and 3. In univariate analysis, the low expression of CASZ1 was a significant risk factor for unfavorable OS ( $p < 0.001$ ), CSS ( $p < 0.001$ ), and PFS ( $p < 0.001$ ). Additionally, a high WHO/ISUP grade and high

T category, N category, and M category were significant risk factors for unfavorable OS, CCS, and PFS. Multivariate analysis was performed with risk factors that were statistically significant on univariate analysis. The CASZ1 expression and high WHO/ISUP grade, T category, N category, and M category were independent prognostic factors for OS, CSS, and PFS.

#### 4. Discussion

In this study, we analyzed the prognostic value of CASZ1 protein expression in ccRCC. We performed immunohistochemical staining of CASZ1 in 896 ccRCC cases and demonstrated that a low expression of CASZ1 was associated significantly with advanced clinicopathologic parameters of ccRCC such as large tumor size, high WHO/ISUP grade, high T category and M category, and high TNM staging. Collectively, our study results show that the low expression of CASZ1 is significantly associated with shorter PFS, OS, and CSS in patients with ccRCC. In multivariate analysis adjusted for nuclear grade and overall stage, the low expression of CASZ1 is an independent prognostic parameter for shorter PFS and CSS of patients with ccRCC.

Great progress has been reported in the research about tumorigenesis, management, and treatment of ccRCC, but little has been discovered about its clinical biomarkers except for the pathologic stage and microscopic necrosis. CASZ1 is a transcription factor, and few studies have revealed the expression of CASZ1 in tumors. In neuroblastoma and HCC, CASZ1 expression was lower in aggressive stage tumors or in cases with poor prognosis [15, 18]. In ovary epithelial cancer, on the other hand, CASZ1 expression was higher in metastatic tumors [19]. These results indicate that CASZ1 has different tumor-specific roles in different tumor types. In ccRCC, based on our study, we suggest that a decreased CASZ1 expression seems to be correlated with tumor progression. To the best of our knowledge, our study is the first to demonstrate the association of CASZ1 protein expression with ccRCC clinicopathologic correlation and prognosis.

Liu et al. suggested that CASZ1 activated pRb in the G1 cell cycle, thus inhibiting cell cycle progression, and reported



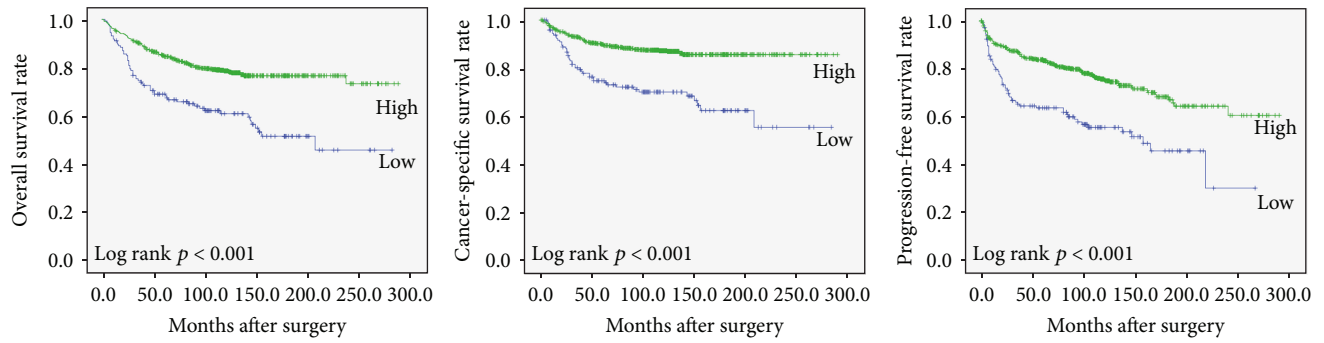


FIGURE 2: Kaplan-Meier curves for impact of the CASZ1 expression on overall survival, cancer-specific survival, and progression-free survival.

TABLE 2: Univariate analysis of overall, cancer-specific, and progression-free survival.

	OS HR (95% CI)	<i>p</i> value	CSS HR (95% CI)	<i>p</i> value	PFS HR (95% CI)	<i>p</i> value
CASZ1						
Low vs. high	0.441 (0.328-0.593)	<0.001	0.363 (0.254-0.518)	<0.001	0.456 (0.342-0.608)	<0.001
Age (years)						
≤55 vs. >55	3.242 (2.383-4.410)	<0.001	2.290 (1.596-3.285)	<0.001	1.852 (1.420-2.415)	<0.001
Gender						
Male vs. female	1.160 (0.845-1.594)	0.359	1.149 (0.771-1.714)	0.494	1.0800 (0.800-1.457)	0.617
WHO/ISUP grade						
1, 2 vs. 3, 4	2.650 (1.994-3.520)	<0.001	6.093 (3.892-9.538)	<0.001	3.034 (2.295-4.012)	<0.001
T category						
T1, T2 vs. T3, T4	3.413 (2.597-4.485)	<0.001	6.012 (4.298-8.4.9)	<0.001	4.822 (3.715-6.259)	<0.001
N category						
N0/Nx vs. N1	8.100 (4.596-14.278)	<0.001	10.984 (6.026-20.018)	<0.001	6.655 (3.710-11.938)	<0.001
M category						
M0 vs. M1	11.088 (8.098-15.182)	<0.001	19.696 (13.821-28.067)	<0.001	15.998 (11.726-21.826)	<0.001

OS: overall survival; CSS: cancer-specific survival; PFS: progression-free survival; HR: hazard ratio; CI: confidence interval.

TABLE 3: Multivariate analysis of overall, cancer-specific, and progression-free survival.

	OS HR (95% CI)	<i>p</i> value	CSS HR (95% CI)	<i>p</i> value	PFS HR (95% CI)	<i>p</i> value
CASZ1						
Low vs. high	0.589 (0.437-0.794)	0.001	0.526 (0.367-0.754)	<0.001	0.558 (0.417-0.747)	<0.001
WHO/ISUP grade						
1, 2 vs. 3, 4	1.775 (1.317-2.391)	<0.001	3.387 (2.129-5.389)	<0.001	1.866 (1.386-2.513)	<0.001
T category						
T1, T2 vs. T3, T4	1.855 (1.378-2.498)	<0.001	2.538 (1.768-3.645)	<0.001	2.431 (1.813-3.259)	<0.001
N category						
N0/Nx vs. N1	5.417 (3.037-9.662)	<0.001	6.190 (3.346-11.451)	<0.001	3.918 (2.157-7.116)	<0.001
M category						
M0 vs. M1	6.497 (4.636-9.105)	<0.001	9.385 (6.429-13.702)	<0.001	7.677 (5.469-10.778)	<0.001

OS: overall survival; CSS: cancer-specific survival; PFS: progression-free survival; HR: hazard ratio; CI: confidence interval.

that in the gene set enrichment assay, CASZ1 repressed MYC target genes in neuroblastoma [23, 24].

Wang et al. suggested that CASZ1 inhibits the MAPK/ERK signaling pathway by downregulating RAF1 in HCC. These authors performed a Cignal Finder Cancer 10-

Pathway Reporter Array experiment and showed that the MAPK/ERK pathway was the most affected. Immunohistochemistry expression of phosphorylated-ERK (p-ERK), MMP2, MMP9, and cyclin D1, which are regulated by the MAPK/ERK signaling pathway, was increased in CASZ1-

silenced cells. Furthermore, these authors demonstrated that CASZ1 inhibits RAF1 protein expression, which is an important element of the MAPK signaling pathway [18]. Furthermore, overexpression of p-ERK is associated with adverse prognosis in RCC [25, 26]. These studies, together with our findings, indicate that CASZ1 can be considered to inhibit RCC progression by inhibiting the MAPK/ERK signaling pathway.

Charpentier et al. suggested that CASZ1 is required for vascular patterning and lumen formation [10, 11, 27, 28]. These authors demonstrated that CASZ1 regulates epidermal growth factor-like domain 7 (Egfl7) and miR-126 to control angiogenesis and vascular remodeling in human cells. CASZ1 positively induces Egfl7 and miR-126 expression in human cells, and so, its depletion leads to altered morphology and cell adhesion in human vascular endothelial cells [10]. Numerous studies have investigated microRNAs (miRNA), which are noncoding RNAs, and their role in the regulation of gene expression [29, 30]. Many of these studies have suggested that miR-126 inhibits cancer cell proliferation and invasion and is correlated with favorable prognosis in various human cancers [31–35]. The low expression of miR-126 is associated with shorter CSS and OS in RCC [36], with metastasis in ccRCC [37, 38], and with therapeutic resistance and cell motility in RCC [39]. The high expression of miR-126 is associated with significantly longer disease-free survival and OS [40] and with low WHO/ISUP grade [41].

## 5. Conclusion

In summary, this study suggests that CASZ1 could be a potential biomarker for predicting the aggressiveness of ccRCC. Further functional studies are needed to validate this role of CASZ1 and to identify the mechanism of CASZ1-mediated tumor progression.

## Data Availability

The data used to support the findings of this study are available from the corresponding author upon request.

## Conflicts of Interest

The authors declare no conflict of interests regarding the publication of this paper.

## Authors' Contributions

Kyung Chul Moon designed the research study. Bohyun Kim and Kyung Chul Moon performed the research. Bohyun Kim and Minsun Jung analyzed the data. Bohyun Kim and Kyung Chul Moon wrote the paper.

## Acknowledgments

This work was supported by grant 03-2015-0230 from the Seoul National University Hospital Research Fund.

## References

- [1] F. Bray, J. Ferlay, I. Soerjomataram, R. L. Siegel, L. A. Torre, and A. Jemal, "Global cancer statistics 2018: GLOBOCAN estimates of incidence and mortality worldwide for 36 cancers in 185 countries," *CA: A Cancer Journal for Clinicians*, vol. 68, no. 6, pp. 394–424, 2018.
- [2] J. J. Hsieh, M. P. Purdue, S. Signoretti et al., "Renal cell carcinoma," *Nature Reviews. Disease Primers*, vol. 3, no. 1, 2017.
- [3] J. Y. Joung, J. Lim, C. M. Oh et al., "Current trends in the incidence and survival rate of urological cancers in Korea," *Cancer Research and Treatment*, vol. 49, no. 3, pp. 607–615, 2017.
- [4] J. R. Srigley, B. Delahunt, J. N. Eble et al., "The International Society of Urological Pathology (ISUP) Vancouver Classification of Renal Neoplasia," *The American Journal of Surgical Pathology*, vol. 37, no. 10, pp. 1469–1489, 2013.
- [5] F. M. Deng and J. Melamed, "Histologic variants of renal cell carcinoma: does tumor type influence outcome?," *The Urologic Clinics of North America*, vol. 39, no. 2, pp. 119–132, 2012, v.
- [6] L. Kuthi, A. Jenei, A. Hajdu et al., "Prognostic factors for renal cell carcinoma subtypes diagnosed according to the 2016 WHO renal tumor classification: a study involving 928 patients," *Pathology Oncology Research*, vol. 23, no. 3, pp. 689–698, 2017.
- [7] R. J. Motzer, E. Jonasch, N. Agarwal et al., "Kidney cancer, version 2.2017, NCCN clinical practice guidelines in oncology," *Journal of the National Comprehensive Cancer Network*, vol. 15, no. 6, pp. 804–834, 2017.
- [8] Z. Liu, X. Yang, F. Tan, K. Cullion, and C. J. Thiele, "Molecular cloning and characterization of human castor, a novel human gene upregulated during cell differentiation," *Biochemical and Biophysical Research Communications*, vol. 344, no. 3, pp. 834–844, 2006.
- [9] R. T. Huang, S. Xue, J. Wang et al., "CASZ1 loss-of-function mutation associated with congenital heart disease," *Gene*, vol. 595, no. 1, pp. 62–68, 2016.
- [10] M. S. Charpentier, K. S. Christine, N. M. Amin et al., "CASZ1 promotes vascular assembly and morphogenesis through the direct regulation of an EGFL7/RhoA-mediated pathway," *Developmental Cell*, vol. 25, no. 2, pp. 132–143, 2013.
- [11] M. S. Charpentier, K. M. Dorr, and F. L. Conlon, "Transcriptional regulation of blood vessel formation: the role of the CASZ1/Egfl7/RhoA pathway," *Cell Cycle*, vol. 12, no. 14, pp. 2165–2166, 2013.
- [12] N. Bhaskaran, Z. Liu, S. S. Saravanamuthu et al., "Identification of Casz1 as a regulatory protein controlling T helper cell differentiation, inflammation, and immunity," *Frontiers in Immunology*, vol. 9, p. 184, 2018.
- [13] Z. Liu, X. Yang, Z. Li et al., "CASZ1, a candidate tumor-suppressor gene, suppresses neuroblastoma tumor growth through reprogramming gene expression," *Cell Death and Differentiation*, vol. 18, no. 7, pp. 1174–1183, 2011.
- [14] Z. Liu, A. Naranjo, and C. J. Thiele, "CASZ1b, the short isoform of CASZ1 gene, coexpresses with CASZ1a during neurogenesis and suppresses neuroblastoma cell growth," *PLoS One*, vol. 6, no. 4, article e18557, 2011.
- [15] R. A. Virden, C. J. Thiele, and Z. Liu, "Characterization of critical domains within the tumor suppressor CASZ1 required for transcriptional regulation and growth suppression," *Molecular and Cellular Biology*, vol. 32, no. 8, pp. 1518–1528, 2012.



- [16] H. Q. Wang, C. Y. Yang, S. Y. Wang et al., "Cell-free plasma hypermethylated CASZ1, CDH13 and ING2 are promising biomarkers of esophageal cancer," *Journal of Biomedical Research*, vol. 32, no. 5, pp. 424–433, 2018.
- [17] A. M. Hoff, B. Johannessen, S. Alagaratnam et al., "Novel RNA variants in colorectal cancers," *Oncotarget*, vol. 6, no. 34, pp. 36587–36602, 2015.
- [18] J. L. Wang, M. Y. Yang, S. Xiao, B. Sun, Y. M. Li, and L. Y. Yang, "Downregulation of castor zinc finger 1 predicts poor prognosis and facilitates hepatocellular carcinoma progression via MAPK/ERK signaling," *Journal of Experimental & Clinical Cancer Research*, vol. 37, no. 1, p. 45, 2018.
- [19] Y. Y. Wu, C. L. Chang, Y. J. Chuang et al., "CASZ1 is a novel promoter of metastasis in ovarian cancer," *American Journal of Cancer Research*, vol. 6, no. 6, pp. 1253–1270, 2016.
- [20] K. Hajian-Tilaki, "Receiver operating characteristic (ROC) curve analysis for medical diagnostic test evaluation," *Caspian Journal of Internal Medicine*, vol. 4, no. 2, pp. 627–635, 2013.
- [21] M. B. Amin, F. Greene, D. R. Byrd, R. K. Brookland, M. K. Washington, J. E. Gershenwald, C. C. Compton, K. R. Hess, D. C. Sullivan, J. M. Jessup, J. D. Brierley, L. E. Gaspar, R. L. Schilsky, C. M. Balch, D. P. Winchester, E. A. Asare, M. Madera, D. M. Gress, and L. R. Meyer, Eds., *AJCC Cancer Staging Manual*, Springer International Publishing: American Joint Commission on Cancer, 8th edition, 2017.
- [22] J. N. S. G. Eble, J. I. Epstein, and I. A. Sesterhenn, *World Health Organization Classification of Tumors: Pathology and Genetics of Tumours of the Urinary System and Male Genital Organs*, IARC Press, Lyon, 2016.
- [23] Z. Liu, J. A. Rader, S. He, T. Phung, and C. J. Thiele, "CASZ1 inhibits cell cycle progression in neuroblastoma by restoring pRb activity," *Cell Cycle*, vol. 12, no. 14, pp. 2210–2218, 2013.
- [24] Z. Liu, N. Lam, E. Wang et al., "Identification of CASZ1 NES reveals potential mechanisms for loss of CASZ1 tumor suppressor activity in neuroblastoma," *Oncogene*, vol. 36, no. 1, pp. 97–109, 2017.
- [25] F. Chen, J. Deng, X. Liu, W. Li, and J. Zheng, "Erratum: Corrigendum: HCRP-1 regulates cell migration and invasion via EGFR-ERK mediated up-regulation of MMP-2 with prognostic significance in human renal cell carcinoma," *Scientific Reports*, vol. 6, no. 1, 2016.
- [26] A. S. Salinas-Sanchez, L. Serrano-Oviedo, S. Y. Nam-Cha, O. Roche-Losada, R. Sanchez-Prieto, and J. M. Gimenez-Bachs, "Prognostic Value of the VHL, HIF-1 $\alpha$ , and VEGF Signaling Pathway and Associated MAPK (ERK1/2 and ERK5) Pathways in Clear-Cell Renal Cell Carcinoma. A Long-Term Study," *Clinical Genitourinary Cancer*, vol. 15, no. 6, pp. e923–e933, 2017.
- [27] M. S. Charpentier, J. M. Taylor, and F. L. Conlon, "The CASZ1/Egfl7 transcriptional pathway is required for RhoA expression in vascular endothelial cells," *Small GTPases*, vol. 4, no. 4, pp. 231–235, 2013.
- [28] M. S. Charpentier and F. L. Conlon, "Cellular and molecular mechanisms underlying blood vessel lumen formation," *BioEssays*, vol. 36, no. 3, pp. 251–259, 2014.
- [29] R. W. Carthew and E. J. Sontheimer, "Origins and mechanisms of miRNAs and siRNAs," *Cell*, vol. 136, no. 4, pp. 642–655, 2009.
- [30] G. J. Hong, V. Kuek, J. X. Shi et al., "EGFL7: master regulator of cancer pathogenesis, angiogenesis and an emerging mediator of bone homeostasis," *Journal of Cellular Physiology*, vol. 233, no. 11, pp. 8526–8537, 2018.
- [31] F. Ebrahimi, V. Gopalan, R. A. Smith, and A. K. Y. Lam, "miR-126 in human cancers: clinical roles and current perspectives," *Experimental and Molecular Pathology*, vol. 96, no. 1, pp. 98–107, 2014.
- [32] Y. Zhou, X. Feng, Y. L. Liu et al., "Down-regulation of miR-126 is associated with colorectal cancer cells proliferation, migration and invasion by targeting IRS-1 via the AKT and ERK1/2 signaling pathways," *PLoS One*, vol. 8, no. 11, article e81203, 2013.
- [33] C. Gong, J. Fang, G. Li, H. H. Liu, and Z. S. Liu, "Effects of microRNA-126 on cell proliferation, apoptosis and tumor angiogenesis via the down-regulating ERK signaling pathway by targeting EGFL7 in hepatocellular carcinoma," *Oncotarget*, vol. 8, no. 32, 2017.
- [34] M. H. Hu, C. Y. Ma, X. M. Wang et al., "MicroRNA-126 inhibits tumor proliferation and angiogenesis of hepatocellular carcinoma by down-regulating EGFL7 expression," *Oncotarget*, vol. 7, no. 41, pp. 66922–66934, 2016.
- [35] W. Zheng, Y. Zhou, J. Lu et al., "The prognostic value of miR-126 expression in non-small-cell lung cancer: a meta-analysis," *Cancer Cell International*, vol. 17, no. 1, 2017.
- [36] L. Gu, H. Li, L. Chen et al., "MicroRNAs as prognostic molecular signatures in renal cell carcinoma: a systematic review and meta-analysis," *Oncotarget*, vol. 6, no. 32, pp. 32545–32560, 2015.
- [37] D. Vergho, S. Kneitz, A. Rosenwald et al., "Combination of expression levels of miR-21 and miR-126 is associated with cancer-specific survival in clear-cell renal cell carcinoma," *BMC Cancer*, vol. 14, no. 1, 2014.
- [38] G. M. Zhang, L. Luo, X. M. Ding et al., "MicroRNA-126 inhibits tumor cell invasion and metastasis by downregulating ROCK1 in renal cell carcinoma," *Molecular Medicine Reports*, vol. 13, no. 6, pp. 5029–5036, 2016.
- [39] W. Liu, H. Chen, N. Wong, W. Haynes, C. M. Baker, and X. Wang, "Pseudohypoxia induced by miR-126 deactivation promotes migration and therapeutic resistance in renal cell carcinoma," *Cancer Letters*, vol. 394, pp. 65–75, 2017.
- [40] H. W. Z. Khella, A. Scorilas, R. Mozes et al., "Low expression of miR-126 is a prognostic marker for metastatic clear cell renal cell carcinoma," *The American Journal of Pathology*, vol. 185, no. 3, pp. 693–703, 2015.
- [41] R. de Cássia Oliveira, R. F. Ivanovic, K. R. M. Leite et al., "Expression of micro-RNAs and genes related to angiogenesis in ccRCC and associations with tumor characteristics," *BMC Urology*, vol. 17, no. 1, p. 113, 2017.